Canine Parvovirus Infection

Events at the Nuclear Envelope and Its Vicinity

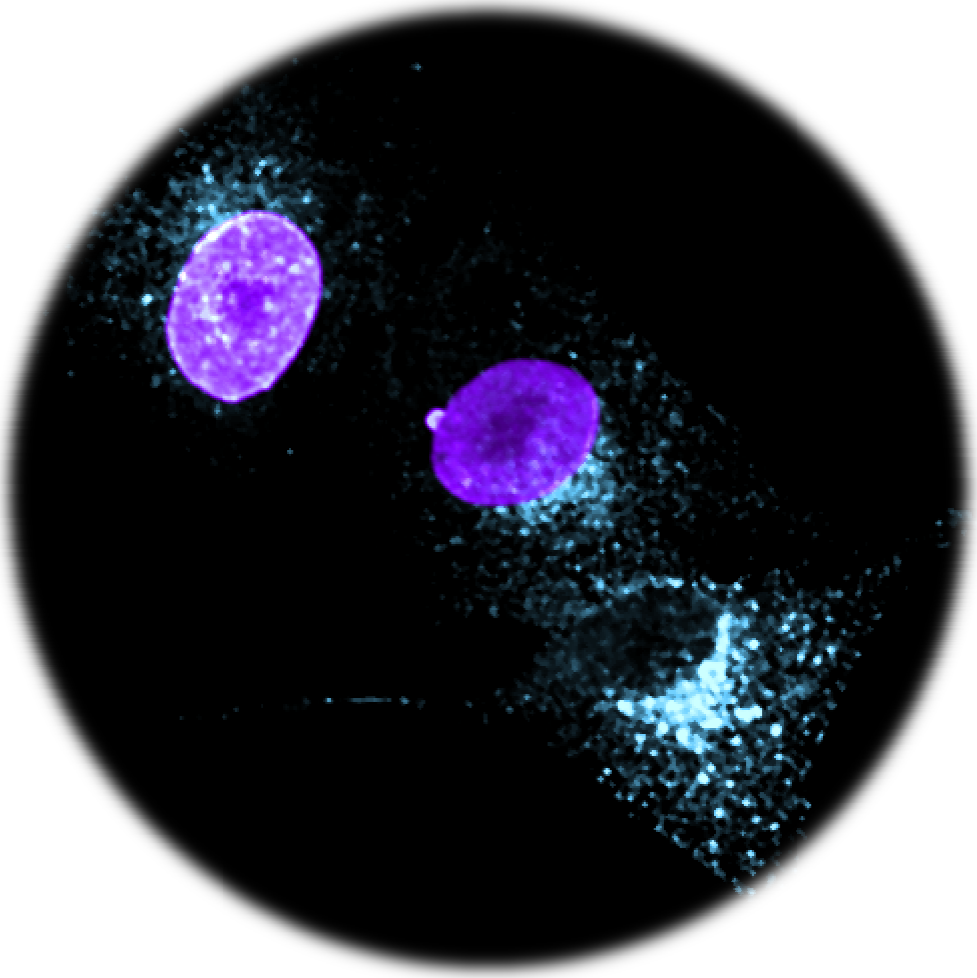

Master´s Thesis
University of Jyväskylä
Faculty of Mathematics and Science
Department of Biological and Environmental Science
Molecular Biology
November 2010
Elina Mäntylä

“Sit down before fact as a little child, be prepared to give up every preconceived notion, follow humbly wherever and to whatever abysses nature leads, or you shall learn nothing”

~ Thomas Huxley, 1860 ~

Preface in Finnish

Tämä Pro Gradu – tutkielma valmistui Jyväskylän yliopiston bio- ja ympäristötieteen laitoksella molekyylibiologian osastolla syyskuussa 2010 useiden kuukausien työvaiheiden jälkeen. Graduaikanani olen saanut nauttia asiantuntevasta opetuksesta ja mahdollisuudesta työskennellä virusten parissa aidossa tutkimusympäristössä. Tästä tilaisuuden ja työvälineiden ojentamisesta tahdon osoittaa suurimmat kiitokseni toiselle ohjaajalleni dosentti Maija Vihinen-Rannalle, jonka kannustuksen, sekä kokemuksen viitottamana olen uppoutunut intohimoisesti tutkimukseen osaamatta – ja haluamatta – enää päästää irti.

Erityiskiitokseni haluan osoittaa myös ohjaajalleni PhD Einari Niskaselle loputtomasta kärsivällisyydestä ja kaikista niistä neuvoista, sekä keskusteluista, joita kävimme tämän tutkielman tekemisen aikana. Asiantuntevan ohjauksensa avulla olen oppinut paljon oman tieteellisen ajattelun kehittämisen tärkeydestä. Kiitän myös tuesta ja itseluottamuksen valamisesta työssä annetun vapaudenkin puitteissa. Haluan kiittää myös PhD Teemu Ihalaista, jonka kannustuksessa ja erinomaisessa ohjauksessa olen oppinut mikroskopiasta, sekä siihen liittyvistä ilmiöistä. Einarin ja Teemun innoittamana olen oppinut tarkastelemaan esitettyjä faktoja kriittisesti. En usko, että unohdan heidän innostustaan tai omistautumistaan tieteelle koskaan.

Hyvästä työilmapiiristä, keskusteluista, vertaistuesta sekä lämminhenkisistä, työhön liittyvien kysymysten ratkaisuista haluan kiittää myös FM Milla Häkkistä, FM Outi Paloheimoa, Olli Kalliolinnaa ja Sami Willmania. Lisäksi kiitän solu- ja molekyylibiologian osaston muuta henkilökuntaa neuvoista ja ongelmatilanteissa saamastani avusta.

Kiitos kuuluu myös vanhemmilleni ja sisarilleni ymmärryksestä ja kannustuksesta. Lopuksi haluan kiittää elämäni tukipilareita, aviopuolisoani Jussia ja pienoista tytärtäni Helmiä, kaikesta siitä rakkaudesta ja tuesta, joita olen teiltä saanut koko opiskeluni ajan. Olette osoittaneet, että kärsivällisyys on hyve.

Jyväskylän yliopisto **Pro gradu – tutkielman tiivistelmä**
Matemaattis-luonnontieteellinen tiedekunta

Tekijä: Elina Mäntylä
Tutkielman nimi: Koiran parvovirus infektio – Tapahtumat tumakalvolla ja sen läheisyydessä
English title: Canine Parvovirus Infection – Events at the Nuclear Envelope and Its Vicinity
Päivämäärä: 30.11.2010 **Sivumäärä:** 49

Laitos: Bio- ja ympäristötieteiden laitos
Oppiaine: Solu- ja molekyylibiologia
Tutkielman ohjaajat: FT Einari Niskanen, Dos. Maija Vihinen-Ranta

---

Tiivistelmä:

Koiran parvovirus (CPV) on vaipaton, negatiivisen, yksijuosteisen DNA-genomin (~5 kb) sisältävä virus. Infektion kulku transferriinireseptorin (Tfr) tunnistuksen ja siihen kiinnittymisen jälkeen jatkuu endosytoosilla ja edelleen viruksen solunsisäisen kuljetuksen avulla kohti tumakalvoa. Pääsy sisälle tumaan on elintärkeää suurimmalle osalle DNA-viruksista, jotta genomi voidaan replikoida. CPV:n ja tumakalvon väliset vuorovaikutukset ovat säilyneet toistaiseksi osittain tuntemattomina. Viimeisimpien tutkimusten mukaan eräät parvovirukset aiheuttavat paikallisia vauroita tumakalvolla. Tumahuokosten (NPC) proteiinien (nukleoporiinit) hajoamista infektion aikana on myös osoitettu tietyillä virustyypeillä.

Tämän tutkimuksen tarkoituksena oli selvittää koiran parvoviruksen toimintaa tumakalvolla ja tämän toiminnan vaikutusta tumakalvon koostumukseen. Työssä tarkasteltiin viruksen aiheuttamia muutoksia tumakalvon ja sitä reunustavan lamiini A/C:n eheydessä, tumahuokosten lukumäärässä ja sen sisältämien proteiinien rakenteissa infektion aikana. Tutkimuksessa pyrittiin myös tarkastelemaan CPV:n kuljetusta sytoplasmassa. Aikaisempien tutkimusten perusteella CPV:n tiedetään hyödyntävän endosomaalista kalvoliikennettä. Tässä tutkimuksessa tarkasteltiin täten myös Rab1A-vesikkelijärjestelmää ja sen roolia viruksen kuljetuksessa infektion aikana.

Tutkimuksen perusteella kävi ilmi, että Rab1A-vesikkelijärjestelmä sijaitsee samoilla alueilla ainakin sisään tulevan viruksen kanssa, mutta virus kulkeutui selvästi eri reittiä pitkin. Tutkimuksesta todettiin, ettei infektion aikana havaittu merkittäviä viruksen aiheuttamia muutoksia tumakalvon tai lamiini A/C:n eheydessä. Myös nukleoporiinit osoittautuivat säilyvän hajottamattomina. Tutkimuksessa ei havaittu nukleoporiinien ja viruksen merkittävää kolokalisoitumista tumakalvolla infektion edetessä. CPV näyttäisi siirtyvän tumahuokoselta tumaan nopeasti kiinnittymättä tumahuokoseen pidemmäksi aikaa. Lisäksi tumahuokosten tiheyden havaittiin pienenevän ja tuman tilavuuden kasvavan kontrolleihin verrattuna infektion seurauksena. CPV infektio näyttäisi joko heikentävän tumahuokosten syntyä tai estävän sitä S-vaiheen aikana.

Avainsanat: Koiran parvovirus, tumahuokonen, nukleoporiini, tumakalvo, lamiini A/C, Rab1A

University of Jyväskylä **Abstract of Master´s Thesis**
Faculty of Mathematics and Science

Author: Elina Mäntylä
Title of thesis: Canine Parvovirus Infection – Events at the Nuclear Envelope and Its Vicinity
Finnish title: Koiran parvovirus infektio – Tapahtumat tumakalvolla ja sen läheisyydessä
Date: 30.11.2010 **Pages:** 49

Department: Department of Biological and Environmental Science
Chair: Cell and Molecular Biology
Supervisors: PhD Einari Niskanen, Dos. Maija Vihinen-Ranta

Abstract:

Canine parvovirus (CPV) is a nonenveloped virus with a linear, negative sense, single-stranded DNA genome of ~5 kb. The infection begins with endocytosis and proceeds via intracellular trafficking of the virus to the nuclear envelope (NE). The nuclear access is essential for most DNA viruses for genome replication. The exact mechanisms of CPV- NE –interactions in infection have remained mostly unknown. Recently, it was shown that some parvoviruses induce local breaks to the NE during infection. There is also evidence of nuclear pore complex (NPC) protein degradation in a virus infection.

The purpose of this study was to unravel the function of CPV on the NE and its components during infection. The approach included observation of the NE, and the nuclear lamin A/C for virus induced conformational changes as well as characterization of the NPC amount and nucleoporin structure in viral infection. One of the aims was also to study the cytoplasmic translocation of CPV. In former studies CPV has been shown to be translocated by using endosomal membrane trafficking during its life cycle. Based on this knowledge the role of Rab1A-associated vesicle system was investigated in this study.

The research indicated that the Rab1A vesicle system locates in the same areas of the cell with the virus at least in the entry, but the virus is clearly trafficked along a separate route. In addition, the results of this study showed no significant virus induced alterations in the conformation of the NE or lamin A/C. The nucleoporins also seemed to stay intact in infection and no colocalization with the virus was detected. It seems that CPV translocates rapidly from the NPCs to the nucleus. However, the NPC density was significantly decreased but the volume of the nucleus enlarged as a consequence of viral infection. It might well be that the CPV infection suppresses the NPC synthesis at the S-phase of the cell cycle or ceases it.

Keywords: Canine parvovirus (CPV), nuclear pore complex (NPC), nucleoporins (Nups), nuclear envelope (NE), lamin A/C, Rab1A

Table of Contents

ABBREVIATIONS

A3B10	Canine parvovirus capsid antibody
APAR-body	intranuclear autonomous parvovirus replication (APAR-) bodies
BSA	bovine serum albumin
Cornell#2	Canine parvovirus capsid protein antibody
CPV	Canine Parvovirus
EGFP	enhanced green fluorescent protein
ERGIC	endoplasmic reticulum-Golgi intermediate compartment
ER	endoplasmic reticulum
HeLa	immortal cell line derived from Henrietta Lacks
Lam	lamin
Mab414	mouse monoclonal antibody against nucleoporins Nup358, 214, 153 and 62
NE	nuclear envelope
NLFK	norden laboratory feline kidney cell line
NPC	nuclear pore complex
NS	nonstructural protein
Nup	nuclear pore complex protein, nucleoporin
pBI265	a plasmid encoding an infective CPV clone
PBS	phosphate buffered saline
PCNA	proliferating cell antigen
Rab1A	Ras related protein
SDS-PAGE	sodium dodecyl sulfate polyacrylamide gel electrophoresis
TfR	transferrin receptor
Tpr	nucleoporin Tpr
TRVb2	CHO derived transferrin receptor deficient cell line
VP	(nonstructural) viral protein

1 INTRODUCTION

1.1 Canine Parvovirus

Canine parvovirus (CPV) was first detected in the mid 1970s and is currently one of the most important pathogens of dogs (Chang, et al., 1992). CPV is a host range variant of feline panleukopenia virus with DNA sequences more than 99 % identical and also a close relative of some other parvoviruses (Reed, et al., 1988, Truyen, et al., 1992). While being characterized as a canine virus it does also replicate in feline, mink (Chang, et al., 1992, Truyen, et al., 1992) and human cells (Parker, et al., 2001). The canine parvovirus host range has been shown to be determined by a specific conformation of an additional region in the threefold spike of the capsid (Parker and Parrish, 1997). CPV is an autonomously replicating virus which replicates only in mitotically active cells (Cotmore and Tattersall, 1987). Thus the infection targets organs that contain actively dividing cells such as in the lymphopoietic system or the intestinal crypt cells (Parrish, 1991, Parker, et al., 2001).

Belonging to the family of *Parvoviridae* and being among the smallest animal DNA viruses, CPV is a nonenveloped virus with a linear, negative sense, single-stranded DNA genome of ~5 kb. The genome has two open reading frames (ORFs) and it encodes four proteins: structural proteins VP1 and VP2, and nonstructural proteins NS1 and NS2. The ORF in the left-hand side of the genome encodes the nonstructural proteins, while the ORF in the right-hand side of the genome encodes the structural proteins. Transcription of structural and nonstructural proteins is initiated from separate promoters. The mRNAs, however have coterminal poly(A) sites and are alternatively spliced (Reed, et al., 1988). In addition, infectious, DNA containing particles include also a protein VP3 produced from VP2 by proteolytic processing (Tsao, et al., 1991).

1.1.1 Capsid Assembly

Nonenveloped canine parvovirus particles are approximately 26 nm in diameter (Tsao, et al., 1991). The icosahedral capsid is assembled from 60 subunits (T=1) of VP1 (~10 %) VP2 (~90 %, Vihinen-Ranta, et al., 2002, Chang, et al., 1992, Tsao, et al. 1991) Full capsids contain also VP3 protein (Weichert, et al., 1998). The three-dimensional structure of the capsid has three different symmetry axes. The surface of the capsid has a 22 ångstrom (Å) long protrusions on the threefold axes (spikes). On the fivefold axel there are

cylindrical, eight-stranded antiparallel β-barrel structures with 15 Å deep canyons circulating them, and 15 Å deep depressions at the twofold axes (Tsao, et al., 1991).

The capsid structure contains also specific receptor binding sites. The detailed mechanisms of virus – TfR-receptor interactions is not yet fully understood but current results suggest that the changes of VP2 residues on the side or top of the threefold spike of the capsid affects the binding to TfR (Hueffer, et al., 2003).

1.1.2 Beginning of infection – the entry

Viral infection is a strictly regulated by series of virus-cell –interactions. Before viruses encounter a target cell, they have to survive outside cells through environmental stresses like changes in temperature and pH, drying and immune defense system. After reaching the cell surface, DNA viruses have to break through the cell plasma membrane, survive endosomal pathways and be transported across the cytoplasm to the nucleus. Final challenge is to import their genetic information through the nuclear envelope inside the nucleus for replication and gene expression. During its life cycle, virus in constantly utilizing various host cell machineries.

Canine parvovirus entry begins with a recognition and attachment to a transferrin receptor (TfR) dimer: a type II membrane protein on the cell surface (Trowbridge, et al., 1986, Lawrence, et al., 1999). TfR is mainly expressed on the basolateral side of the polarized epithelial cells (Trowbridge, et al., 1986, Basak and Compans, 1989). Rapid, receptor-mediated endocytosis takes place after receptor binding. Internalization of CPV is a clathrin-mediated and dynamin-regulated process (Parker and Parrish, 2000) followed by the nuclear targeting of the viral capsid.

Cytoplasmic trafficking following the internalization is a process that has remained partly unclear. It is known that a productive infection includes at least microtubule-dependent capsid transport in endosomes (Vihinen-Ranta, et al., 1998). It has been suggested that the CPV capsids are transported from the early to the recycling endosomes and pass through late endosomes to the lysosomes (Suikkanen, et al., 2002). The low pH of endosomal vesicles induces conformational changes in the viral capsid (for review see Harbison, et al., 2008). These changes are essential for accomplishing the entry and releasing the viral particle into the cytoplasm from prelysosomal endosomal vesicles (Vihinen-Ranta, et al.,

1998, Parker and Parrish, 2000, Suikkanen, et al., 2003I). It is known that the VP1 N-terminal sequence affects endosomal release and nuclear transport of capsids (Vihinen-Ranta, et al., 2002). The lipolytic PLA_2-activity of VP1 has been shown to affect the endosomal vesicular membrane disruption and facilitate the viral escape into the cytoplasm (Farr, et al., 2005).

The cytoplasmic route from vesicle escape to the nuclear pore complexes (NPCs) and release of the genome to the nucleus are still poorly understood. Transport of CPV to the perinuclear area has been shown to be dependent on the physiological temperature and on the intact microtubules (Vihinen-Ranta, et al., 2000). It is also known that the capsids are retained in endosomal or lysosomal vesicles for several hours (from one to over six hours, Suikkanen, et al., 2002, Parker and Parrish, 2000, Harbison, et al., 2009).

VP1, one of the CPV capsid proteins, has a unique nuclear localization signal (NLS) region. Results show that this N-terminal sequence of VP1 with several basic amino acids seems to control the nuclear transport after the vesicular escape and is required for successful infection (Vihinen-Ranta, et al., 2002). It seems that the capsids are trafficked via microtubules into close proximity of the nuclear pore complexes before entering the nucleus in intact form (Vihinen-Ranta, M., et al., 2000).

1.1.3 Gene expression and genome replication

In the nucleus the single-stranded DNA of canine parvovirus is converted to a double stranded DNA (dsDNA) which allows transcription by the host transcriptional machinery. In the nucleus the viral genome is also expressed leading to progeny virus production including capsid assembly and packaging of the genome into new capsids.

The parvoviral genome is replicated through modified rolling-circle mechanism. NS1 initiates replication by binding with replication-essential high-mobility-group proteins (Cotmore and Tattersall, 1998) to the right-hand origin, and with glucocorticoid modulatory element-binding proteins to the left-hand origin (Christensen, et al., 1997). Both recognitions lead to the ATP dependent nicking of the viral DNA. NS1 stays attached to the 5´end of the genome and the 3´end serves as a starting point for primers to form in nascent strand synthesis (Cotmore and Tattersall, 1988). In the next phase NS1 has a role as an ATP-powered helicase in resolving terminal hairpin structures (Willwand, et al.,

1997) and unwinding the DNA. Besides NS1 also at least polymerase δ and a replication protein A are involved in the process (Christensen and Tattersall, 2002).

1.1.4 Release from the host – the egress

Viral infection leads to several functional and morphological alterations in the host cell, often culminating in cell death and lysis. One example of the dramatic changes is the intranuclear autonomous parvovirus replication (APAR-) bodies. APAR-bodies function as parvoviral DNA replication centers and are defined by the existence of NS1 (Cziepluch, et al., 2000). APAR-bodies are formed early in infection emerging first as small foci in the interchromosomal domains at ~12 h p.i. and finally filling most of the nucleus at ~24 h p.i (Cziepluch, et al., 2000, Ihalainen, et al., 2007, Ihalainen, et al., 2009).

Some of these changes may help the progeny virus particles to be released. In late phases of the parvovirus infection changes in the cytoskeleton are detected. This leads to rounding-up of the cells followed by detachment from the growth platform (Herrero, et al., 2004). In addition, changes of cytoskeletal filaments like actin or tubulin have been reported (Bär, et al., 2008, Pakkanen, et al., 2008). The dependence of a multifunctional, actin-severing and capping protein gelsolin in remodelling of the actin-network, virus transport from nucleus to the cell periphery and in release from the host cell has been proven in minute virus of mice (MVM) studies (Bär, et al., 2008).

Furthermore, the export of new progeny viruses through cytoplasm has been suggested to be guided by the cytoskeleton and mediated by lysosomal or late endosomal vesicles challenging the former view that the release of autonomous parvoviruses is a passive process (Bär, et al., 2008). Parvoviruses are commonly released from the cells via cytolysis triggered by multiple factors in infection (Nuesch and Rommelaere, 2006) although there is some evidence of parvovirus release in the absence of cell lysis (Lachmann, et al., 2003).

1.2 Cell – a basic unit of life

All living organisms, though infinitely varied when viewed from the outside, have something in common: the basic unit of life and living matter – the cells. Cells share almost the same machinery for their basic functions but yet they carry the most astonishingly diverse genetic material determining the unique differences between individual beings. The smallest organisms consist of single cells and the largest, multicellular organisms contain different types of cells differing in size, shape and specialized function. The higher organisms have their genome enclosed within a double membrane, the nuclear envelope, and this compartment is called the nucleus. Cells with nuclear envelopes are called eukaryotes. Those cells without nuclear envelopes are bacterial cells, prokaryotes (Alberts, et al., 2002).

Viruses take advantage of the highly organized machineries of the cells during their life cycle. Having small genomes containing only the essential information in the form of DNA or RNA, viruses use the host cell´s transcriptional and translational machineries for their replication during infection.

1.2.1 Nuclear Envelope

A barrier that separates the nucleus from the cytoplasm and encloses the DNA in a cell nucleus is the nuclear envelope (NE). NE consists of a double-bilayer of lipids with a diverse array of proteins embedded in it (for review see Hetzer, et al., 2005). Embedded in the NE are also the nuclear pore complexes (NPCs), large protein assemblies that regulate bidirectional transport of molecules, including proteins and mRNAs, between the nucleus and the cytoplasm (Pantè and Kann, 2002). NE is also directly connected to the extensive membranes of the endoplasmic reticulum. Underlying the double-bilayer of lipids there is a meshwork-like proteinaceous lamina (for review see Gruenbaum, et al., 2005).

Besides functioning in the molecular trafficking NE provides an important regulatory level into the eukaryotic cell by separating transcription and translation spatially to nucleus and cytoplasm, respectively. Nucleus has allowed splicing to become an important process in eukaryotic gene function (Cohen and Pante, 2005). NE also provides structural anchoring sites for components including chromatin and the cytoplasmic filaments (Gerace and Blobel, 1982). Recent studies indicate that the periphery of the nucleus provides a platform

for sequestering transcription factors and the nucleoplasmic side of the NE can function as a resting place for some transcription factors (for review see Heessen and Fornerod, 2007).

In mitosis, NE break down (NEBD) in the end of the prophase is required to allow cell division. The earliest event of NEBD is an increase in the permeability of the nuclear envelope coinciding with the dissociation of some nucleoporins from the NPCs (Kiseleva, et al., 2001). It has been speculated that there are some alterations in the structure or conformation of the NE also during viral infection. There is evidence that at least one other parvovirus, MVM, introduces damage to the NE when microinjected into Xenopus oocytes (Cohen and Pante, 2005). It is also known that during certain virus infections (like poliovirus, a RNA virus) the efflux of some nuclear proteins is facilitated (Belov, et al., 2004). It has also been shown that the NE permeability is altered in CPV infection (Teemu Ihalainen, unpublished).

1.2.2 Nuclear Pore Complex

Nuclear pore complexes (NPCs) are large, ~125 MDa, proteinaceous structures consisting of approximately 30 protein species called nucleoporins (Nups). Each Nup is present in 8-48 copies due to the eight fold symmetry of the NPC (Figure 1). On the cytoplasmic side NPC has eight fibers protruding from a ring-like central pore structure. The central pore is approximately 90 nm in length and 45-50 nm in diameter at the NE midplane. Also on the nucleoplasmic side, eight fibers extrude forming a cage-like structure (distal ring) of the nuclear basket (for review see Fahrenkrog, et al., 2004). The central ring forms an aqueous opening in NE allowing transportation of cargos with maximum diameter of ~39 nm (Pantè and Kann, 2002). NPC structure seems to be fairly conserved from yeast to higher eukaryotes with certain differences in linear dimension (for review see Fahrenkrog, et al., 2004).

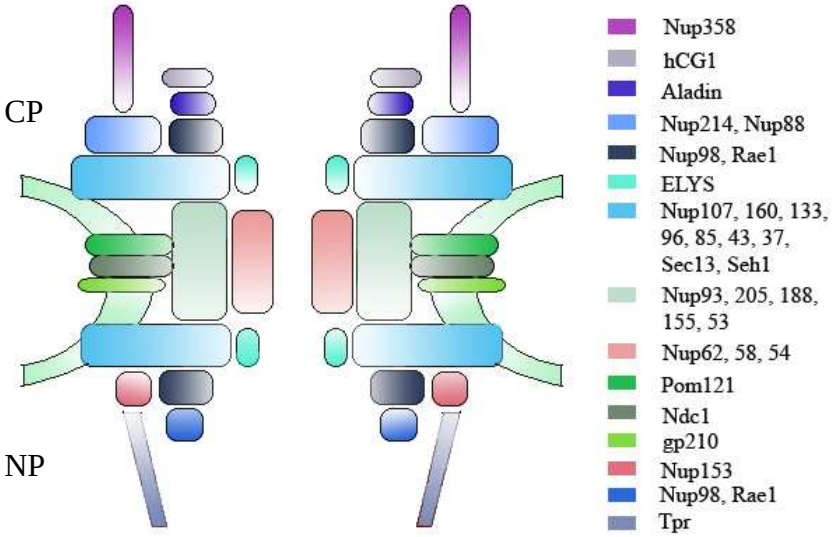

Figure 1. Structure of the NPC. Reconstruction of a NPC structure diagram (modified from Antonin, et al., 2008) with a schematical presentation of different nucleoporin locations. Cytoplasm (CP), nucleoplasm (NP).

NPCs function as gateways in all nucleocytoplasmic transport pathways by allowing the free diffusion of ions and small, less than ~9 nm in diameter, molecules (Paine, et al., 1975). In addition, it is involved in receptor-mediated transport of macromolecules such as proteins, RNAs and ribonucleoprotein particles. The traffic of macromolecules is accomplished by dedicated carriers recognizing nuclear localization and export signals (for review see Fried and Kutay, 2003). The phenylalanine-glycine (FG) repeats of Nups seem to be essential for this movement which can occur against a concentration gradient of the carried molecules (for review see Fahrenkrog, et al., 2004).

1.2.3 Nucleoporin Tpr

The function of a 265 kD nuclear pore protein Tpr (translocated promoter region) (Mitchell and Cooper, 1992) is controversial. It has been suggested to have a role in intranuclear and nucleocytoplasmic transport, especially in export (Frosst, et al., 2002). General function of Tpr as a scaffold protein has been under debate. However, the latest studies have shown that NPCs are formed in the absence of Tpr. This suggests that Tpr is not mandatory for NPC assembly (Hase and Cordes, 2003). Recently it was shown that Tpr has a central function as a determinant of perinuclear organization and in delimiting heterochromatin distribution (Krull, et al., 2010).

Tpr localizes to the nuclear basket of the NPC within ~120 nm of the pore midplane, where it is thought to have an architectural role (Frosst, et al. 2002, Krull, et al., 2004). It has also been proposed to reside in the filaments which extend from the nuclear basket into the nuclear interior (Cordes, et al., 1997) but there is evidence suggesting that this may not be the case (Frosst, et al., 2002).

1.2.4 Nup153

Nup153 has been shown to be a direct binding partner that links Tpr to the NPC central pore in mammals and is crucial for the incorporation of various other nucleoporins to NPC (Hase and Cordes, 2003, for review see Fahrenkrog, et al., 2004). It is located at the nucleoplasmic side of the nuclear basket, in an area occupied by the nuclear coaxial ring, and it interacts with transport factors suggesting a role in nucleocytoplasmic transport (Shah, et al., 1998, Stoffler, et al., 1999, Krull, et a., 2004). This is supported by data showing interaction between Nup153 and the import complex of cargo and importins (Shah, et al., 1998, Schmitz, et al., 2010). Nup153 has been shown to arrest Hepatitis B virus capsids in the nuclear basket during infection (Schmitz, et al., 2010).

1.2.5 Nup358

Nup358 (RanBP2) resides on the cytoplasmic filaments of the NPC in the interphase cells. It is also seen in some amounts in the mammalian cytoplasm, where it particularly enriches to cell extensions (Walther, et al., 2002, Joseph, et al., 2004). The association of Nup358 to the NPC filaments is dependent on interactions with Nup214 and Nup88 (Bernad, et al., 2004). Cytoplasmic Nup358 often colocalizes with microtubules (Joseph and Dasso, 2008). In metaphase, this large nucleoporin localizes to mitotic spindles and kinetochores and is therefore important for microtubule-kinetochore interactions. In another words, Nup358 is controlling the microtubule cytoskeleton - for example its assembly (Joseph, et al., 2004).

Studies have revealed that Nup358 both provides a platform for rapid disassembly of transport receptor (CRM1) complexes and a binding site for empty transport receptor recycling into the nucleus. It has also been shown that the removal of Nup358 causes a distinct reduction in nuclear export signal-dependent nuclear export (Bernad, et al., 2004).

1.2.6 Nuclear lamin A/C

Nuclear lamin is a proteinaceous, cytoskeletal structure that is lying underneath NE. It is composed of lamin filaments, which belong to the type V intermediate filament family, and lamin associated proteins (Gruenbaum, et al., 2005). It is closely connected with both the inner nuclear membrane and the chromatin (Stewart, et al., 2007). Lamin provides anchoring sites for the NPCs and confers structural and mechanical stability to the NE (Gerace, et al., 1988). In addition, nuclear lamin has a role in apoptosis and is needed in DNA replication, proper cell cycle regulation, chromatin organization and cell differentiation. It was also discovered recently that some genetic diseases are caused by mutations in the proteins of the nuclear lamina. Underlying mechanisms causing the disesase were found to be defects in cell mechanics, polarization and migration (for review see Hutchison, 2002, Lee, et al., 2007). Lamin filaments constitute the type V intermediate filament family. In mammals, the alternative splicing of a single gene encodes A-type lamins (lamin A, AD10, C2), while B-type lamins (B1, B2, B3) are encoded by two distinct genes. A-type lamins are developmentally regulated. B-type lamins are essential for cell viability (for review see Hutchison, 2002).

1.2.7 The ER-Golgi intermediate compartment and Rab1A

Connected to the NE in the cytoplasm is the endoplasmic reticulum (ER). Between the rough ER and the Golgi apparatus resides the ER-Golgi intermediate compartment (ERGIC) composed of a complex labyrinth of membranes and proteins. Despite of its location, the protein composition of the ERGIC membranes differs from the membranes found in the ER and Golgi (Scweizer, et al., 1991).

The ERGIC contributes to the concentration, folding, and quality control of newly synthesized proteins. It also generally functions in vesicular protein trafficking between the ER and the Golgi and may present the first post-ER sorting mechanism (for review see Appenzeller-Herzog and Haurl, 2006). One of the sorting types of this system is a Rab-dependent, vesicular coat protein COPI-mediated sorting through Rab effectors. Rab-mediated trafficking in ERGIC is bidirectional and involves two different Rab molecules, Rab1 and Rab2. The Rab1 is involved in membrane tethering at the ERGIC and cis-Golgi in anterograde transport and in COPI recruitment (Allan, et al., 2000).

2 AIMS OF THE STUDY

Viral infection in general leads to several functional and morphological alterations of the host cell. Evidence of parvovirus induced dramatic changes in NE morphology and the structure of its components has been stated in former studies. In this study, the previously characterized CPV –induced effects were investigated. In addition, the endosomal membrane associated trafficking of CPV has remained partly unknown. This research was accomplished also to enlighten the events of this trafficking.

2.1 Specific aims of the study

1) To elucidate the effects of CPV infection on the structure of NE by monitoring the amount of the NPCs and possible degradation of the Nups.
2) To monitor lamin A/C and the NE during viral entry for virus induced conformational alterations.
3) To elucidate the possible role of the ER intermediate compartment in CPV nuclear entry and egress.

3 MATERIALS AND METHODS

3.1 Cells and viruses

Norden Feline Laboratory Kidney (NLFK) and HeLa MZ (CCL-2) cells were cultured in Dulbecco`s Modified Eagle`s medium (DMEM, Gibco, UK) supplemented with 10 % fetal bovine serum (FBS) (Gibco, Paisley, UK), 1 % non-essential amino acids (Gibco, Paisley, UK), 1 % Penicillin-Streptomycin (Gibco, Paisley, UK) and 1 % L-Glutamin (Gibco, Paisley, UK) at +37 °C in a humidified incubator with 5 % CO_2. NLFK cell line stably expressing lamin C-EGFP was maintained in a medium also supplemented with selective antibiotic Geneticin 418 (0.4 mg/ml G418, Sigma Chemical Co., Germany). Transferrin receptor negative TRVb2 cells (Vogt, et al., 2003, McGraw, et al., 1987) were cultured in standard F12 Ham (Gibco, Paisley, UK) supplemented with 5 % FBS (Gibco, Paisley, UK), 1 % Penicillin-Streptomycin (Gibco, Paisley, UK) and 1 % L-Glutamin (Gibco, Paisley, UK). All cell types were grown in a monolayer in 75 cm^2 culturing flasks (Sarstedt Inc., Newton, USA) and passaged twice a week.

For immunolabeling and Western blot the cells were grown to approximately 80-90% confluency either on coverslips (13 mm in diameter) or on dishes (35 mm in diameter) the medium was changed and the cells were infected on dish with CPV in growth media. 100 µl of virus suspension was added and incubated in +37 °C/5 % CO_2 incubator for indicated time (0.5 – 72 h). For immunolabeling the cells were washed with phosphate buffered saline (PBS, 0.02 M sodium phosphate buffer with 0.15 M sodium chloride, pH 7.4) and fixed with paraformaldehyde (4 % PFA in PBS) for 20 minutes. Cells were again washed with and stored in PBS (+4 °C) until immunolabeling. For Western blotting cells were washed with PBS, incubated with trypsin (Gibco, Paisely UK) until completely detached, centrifuged (500 x g, 5 min, Eppendorf centrifuge 5415D) and resuspended in 100 µl of PBS.

For live cell imaging cells NLFK-LamC-EGFP cells were cultivated in 90% confluence on live imaging dishes (50 mm in diameter) featuring a glass-bottom circular opening (10 mm) cut into center of the attachment surface (MatTek Corporation, Ashland, USA) and either microinjected with CPV supplemented with red Dextran (Rhodamin, Fritch, 1:1, 0.9 mg/ml) into the nuclei or cytoplasms or infected with CPV in growth media (100 µl or

1000 µl to increase M.O.I., respectively). The microinjections were accomplished by using a system comprised of Transjector 5246 and a Micromanipulator 5171 (Eppendorf, Hamburg, Germany) on an Olympus IMT-2 inverted microscope. Needles were pulled from glass capillaries (Clark Electromedical Instruments, Reading, UK) using a P-97 needle puller (Sutter Instruments, Novato, CA).

Rab1A-EGFP and pBI265 plasmid transfections were performed to NLFK and TRVb2 cells with TransIT-LT1 reagent (Thermo Fisher Scientific Inc, Waltham, MA) according to the manufacturer's protocol.

3.2 Induction of apoptosis

Cells were cultivated until 80-90 % confluence on 35 mm dishes. Following medium change either staurosporin (1 µg/ml, Sigma-Aldrich, St. Louis, USA) or actinomycin-D (0.5 µg/ml, Sigma-Aldrich, St. Louis, USA) diluted in DMEM was added to induce apoptosis and incubated in +37 °C/5 % CO_2 incubator for 1, 2, 4, 6, or 24 h. After incubation cells were washed once with PBS, trypsinized (+37 °C) until completely detached, pelleted (500 x g / 5 min, Eppendorf centrifuge 5415D), resuspended in PBS (100 µl) and stored (+4 °C).

3.3 SDS-Page and immunoblotting

Suspensions of variously treated NLFK and HeLa cells in PBS (100 µl) were mixed with equal volumes of SDS-Page Sample buffer and boiled for 10 minutes. Samples were stored in -20°C. For Western blot, the protein separation electrophoretically by sodium dodecyl sulfate polyacrylamide gel (8 %) electrophoresis (SDS-Page) onto nitrocellulose and immunoblotting were done by using standard methods. In immunoblotting the antibodies were diluted in 5 %-milk-TBS-Tween-20 (1 %). Supersignal® West Pico Chemiluminescent Substrate (1:1, Thermo Scientific) was used for visualization of proteins. Signal was collected quantitatively with a Chemidoc XRS (Bio-Rad, UK).

3.4 Immunolabeling

Cells on coverslips were first incubated with permeabilization buffer (1 % BSA, 0.1 % Triton-X-100 and 0.01 % NaN_3, 20 min). Primary antibodies diluted in 3 % BSA-PBS were added and incubated for 1 h in room temperature. After series of washes first with

permeabilization buffer (15 min, RT), PBS (15 min, RT) and again with permeabilization buffer (15 min, RT) the coverslips were incubated with secondary antibodies for 30 minutes (RT) in the dark. Finally the samples were rinsed with permeabilization buffer (15 min, RT) and with PBS (15 min, RT). The samples were projected from the light during the washes and embedded in Mowiol containing Dabco antifade reagent (30 mg/ml, Sigma-Aldrich, St. Louis, USA) or DAPI (ProLong Gold antifade reagent with DAPI, Invitrogen, Eugene, Oregon, USA).

3.5 Antibodies

Mouse monoclonal antibodies against the N-terminus of Nup153 (1:500, 1 mg/ml, ab24700-100) and nucleoporin antibody Mab414 (1:5000, 1 mg/ml, ab24609) were from Abcam (Cambridge, UK). Rabbit antibodies against the C-terminus of Tpr (IF: 1:200, WB: 1:500 and 1:250, ab84516) and against the N-terminus of Nup358 (1:1000, ab64276) were purchased from Abcam (Cambridge, UK). For visualization of lamin A/C a mouse antibody αLam A/C (1:100, NCL-LAM-A/C, Novocastra, UK) was used. Rabbit αPCNA (1:500, ab18197, Abcam, Cambridge, UK) was used as an infection marker. For detecting CPV capsids mouse antibody A3B10 (1:200) and Cornell #2 (1:800) were utilized (gifts from Colin Parrish, Cornell University, Ithaca, N. Y.). Goat anti-mouse or anti-rabbit Alexa488, 555 and 633-conjugated secondary antibodies were used (1:200, Molecular Probes, Eugene, OR, USA). In immunoblotting the secondary antibodies used were horseradish peroxidase-conjugated goat anti-rabbit or anti-mouse igG (1:2000, Pierce Biotechnology, Rockford, IL).

3.6 Confocal microscopy

3.6.1 Fixed-cell imaging

Fixed cell confocal microscopy was conducted with Olympus FluoView FV 1000 confocal laser scanning microscope using 60x oil immersion objective (UPLSAPO 60x / numerical aperture [NA] = 1.35, oil immersion).

For the visualization and estimation of the number of nuclear pores and nuclear surface areas (with αNup153 and αPCNA) argon laser with excitation wavelength of 488 and HeNe laser with the excitation wavelength of 543 were used, respectively. The emissions

were detected with 500- to 530-nm-band-pass and 555- to 655-nm-band-pass filters. Image size was 512 by 512 pixels. Step Size (slice size, nm/slice) was 150 nm and the number of slices in a stack varied from 25 to 35. The pixel size (X/Y) was 51 nm with optical resolution of 172 nm. Sequential scanning was used. Pinhole was adjusted to 50. The fluorescent images were taken without the DIC prism and averaging.

In simultaneous imaging of microinjected CPV and stained Nup358, or in Rab1A-EGFP studies in fixed, Argon laser with the excitation wavelength of 488 (for Lam A/C-eGFP or Rab1A-EGFP), and HeNe laser with the wavelengths of 543 (for A3B10) and 633 (for Nup358) were used. The emissions were detected with 500- to 530-nm-band-pass (EGFPs), 555-to 625-nm-band pass (A3B10 in microinjection studies), 555- to 655-nm-band-pass (Rab1A-EGFP) and 650-nm-long-pass filters. Pixel size was 60-70 nm. In stack the step size was 150 nm. Picture size varied from 512 by 512 and 800 by 800 to 1024 by 1024. During scanning the used averaging was Kalmann (value of 2-4).

3.6.2 Live-cell imaging

In live-cell microscopy the images were acquired with Zeiss CellObserver HS widefield microscope (Zeiss, Göttingen, Germany) with a 63x glycerol immersion objective (Plan Neofluar 63x / numerical aperture [NA] = 1.30, glycerol immersion). The microscope incubator was maintained in +37 ºC during observation and the CO_2 concentration was adjusted to 5 %. Used excitation leds were 470 nm and 509 nm from a Colibri light source (Zeiss). The fluorescence was collected with a Zeiss AxioCam MRm. Binning (2 x 2) was used to reduce the exposure time (maximum of 800 ns). Imaging started immediately post infection. Frame rate varied from 12 to 4 frames per hour and imaging session durations raised from 1 to 24 h.

3.7 Image analysis

After imaging, the acquired data was analyzed with ImageJ program (ImageJ 1.44d, Abramoff, et al., 2004). Tables were constructed in Microsoft Excel. Image panels were constructed in Adobe Photoshop® CS2.

3.7.1 Estimation of the number of NPCs

For calculating the amount of nuclear pores in a sample cell, the acquired data included two channels: 488 nm laser for αNup153 (NUP channel) and 543 nm laser for αPCNA (PCNA channel). From αNup153 fluorescence image stack, the slice with the whole bottom of the cell and the best possible array of nucleoporins was first located. Then, an average intensity projection from a few slice before and after was calculated. To reduce the noise, Gaussian filtering with the radius of one for the NUP channel, and a median filtering with a radius of one for the PCNA channel, respectively. The nucleus was thresholded using the median filtered, average intensity PCNA channel and used as the area of nucleus. By using the specific area of the nucleus the amount of NPCs was calculated by using the find maxima –command in the “Process” –menu of ImageJ. A suitable noise tolerance value for this application was gained through trials performed uniquely for each sample cell.

3.7.2 Analysis of nuclear surface area and volume

After median filtering (radius 1) the moderated αPCNA channel stack used in the NPC amount estimations was thresholded and the nuclear area was measured. For the volume determination the original αPCNA or αLam A/C fluorescence stack was thresholded after median filtering (radius 2). The volume of the nucleus was measured with an ImageJ 3D-Objects counter plugin. The used voxel size was 51 nm x 51 nm x 150 nm in acquiring of the data.

3.7.3 Localization studies

For studying the possible localization and colocalization of the fluorescent proteins used in this study the acquired data was analyzed and enhanced. Depending on the use of the source data, the z-projects (average intensity for stacks) of the images were used and/or the images were modified with the Gaussian filtering (radius 1). In addition, the brightness and contrast were adjusted.

4 RESULTS

4.1 Effects of CPV infection on the structure of NE

To analyze the molecular structure of the NE during infection, the density of one of its components, the nuclear pores, was estimated in infected and compared to that of noninfected NLFK cells in S- or G –phase (G_1/G_2) of the cell cycle. Nucleoporin antibody against Nup153 was used to detect the nuclear pores, and αPCNA was used as a marker for recognizing infected cells as well as the S- or G –phase in the noninfected cells. The nuclear basal surface area was measured in ImageJ by using the αPCNA labeling. The fluorescence staining was bright and separate Nup153 labeled spots clearly detectable. Confocal microscopy did not directly show any detectable differences in the NPC densities between samples. Computer analysis, however, showed a statistically significant decrease in the density of the NPCs in CPV infected compared to the control cells (Student´s t-test; p=0.003). The density of NPCs in infected cells (2.45 ± 0.60 NPC/μm^2) was ~30 % lower than in non-infected G-phase and S-phase cells (3.57 ± 0.31 and 3.36 ± 0.88 NPC/μm^2). There was no statistically significant difference in the densities of NPCs in S- or G.phase cells (p=0.309) (Figure 3). The nuclear surface area at the basal side of the infected cells (198.98 μm^2) was ~23 % larger than in the G-phase control cells (160.48 ± 29.49 μm^2) (Figure 2). Small, but statistically insignificant increase in nuclear surface area was also detected when comparing infected and non-infected S-phase cells (172.97 ± 29.90 μm^2) (Figure 3).

To analyze CPV induced effects on the structure of the NE, degradation of certain nucleoporins was studied in NLFK and HeLa cells infected with CPV or induced in apoptosis with staurosporin or actinomycin D. Western blots of variously treated cells were accomplished with nucleoporin antibody Mab414 (Figure 4) and nucleoporin specific antibodies against Nup153, Nup358 (Figure 5) and Tpr (data not shown) used in detection. No partial or full degradation of nucleoporins studied in either infected (24 h p.i.), control, or apoptosis induced cells was observed in this study (Figure 4,5,6).

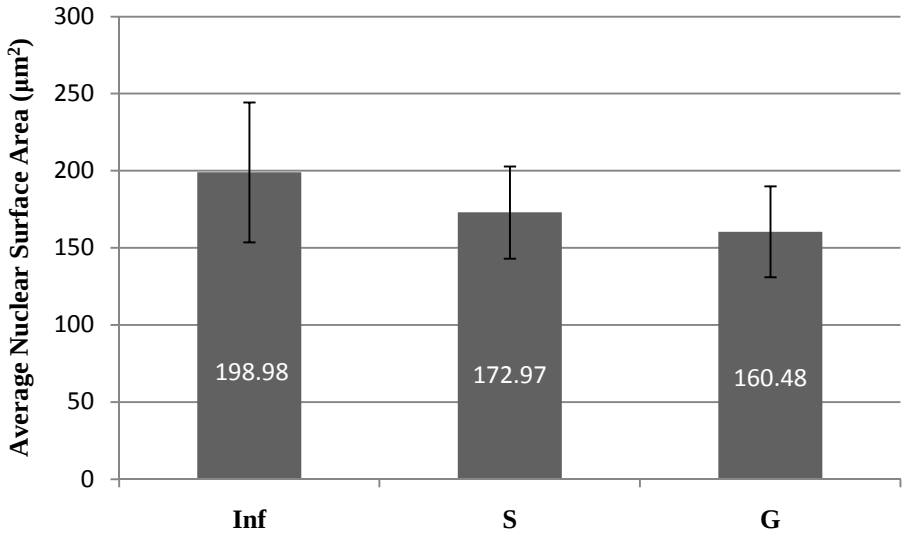

Figure 2. Average nuclear basal surface areas of the infected and control NLFK cells. A statistically significant increase in the nuclear surface area during infection compared to the control cells in G-phase of the cell cycle. Nuclear surface area was determined via αPCNA labeling in confocal microscopy. Error bars indicate the standard deviations.

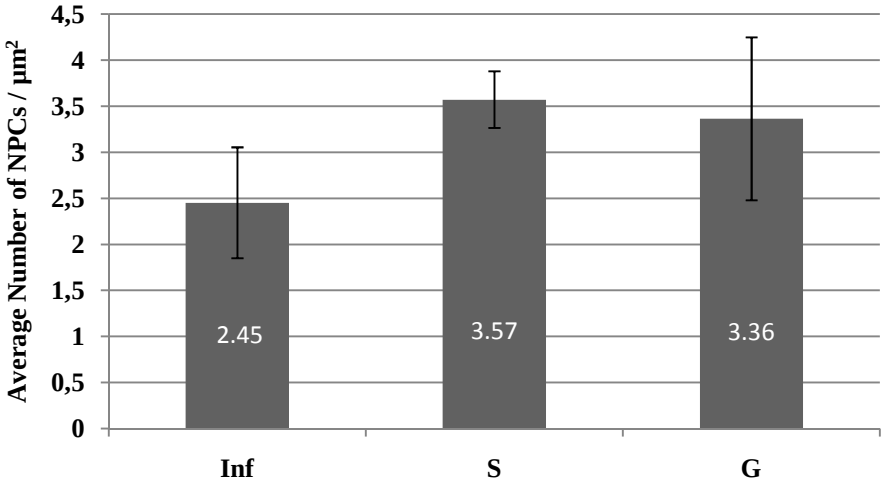

Figure 3. Average nuclear pore complex densities (number of NPCs/µm2) in infection (24 h p.i.) and in S- or G-phase control cells. The density of NPCs decreases significantly as a consequence of CPV infection. Error bars indicate the standard deviations.

4.2 Nuclear volume increases slightly in CPV infection

Since nuclear basal surface is dependent on cell shape, we wanted to use 3D analysis to study possible infection induced changes in the nuclear volume. To this end, cells were labeled with αPCNA or/and αLam A/C antibodies and imaged with confocal microscopy. Computer analysis of the nuclear volume was applied to filtered and thresholded image stacks with 3D-Object Counter particle analysis plugin in ImageJ. The results obtained with αPCNA showed a statistically significant increase (~21 %, p=0.03) in the nuclear volume in CPV infected NLFK cells (464.05 ± 116.02 μm^3) in relation to G-phase control cells (384.81 ± 120.79 μm^3). The increase in volume was observed also when compared to S-phase cells but this difference was not significant (~4 %) (Figure 14). Measurements accomplished with the αLam A/C labeling showed a small increase in CPV infected cell nuclei size compared to the controls but the differences were not significant.

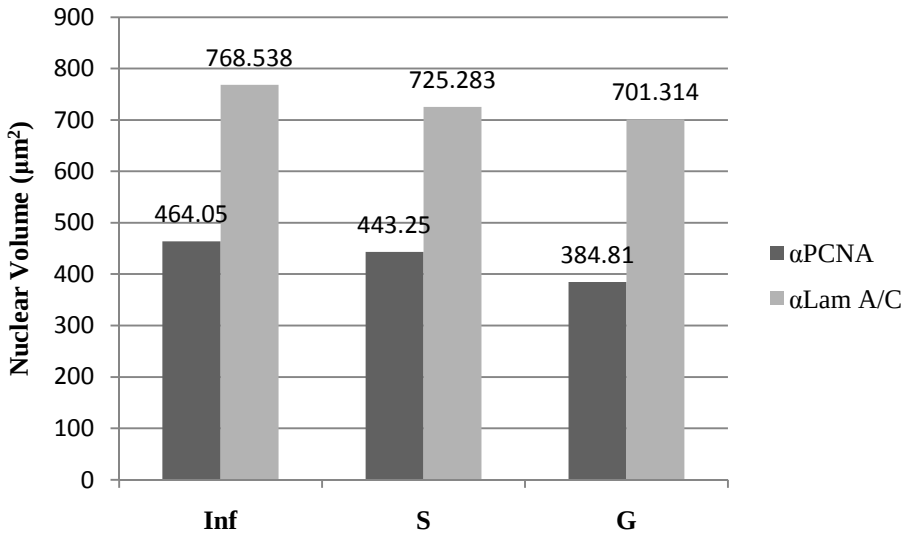

Figure 14. Average nuclear volumes measured with αPCNA labeling of the CPV infected and control NLFK cells. A statistically significant increase in the nuclear volume during infection compared to the control cells in G-phase of the cell cycle.

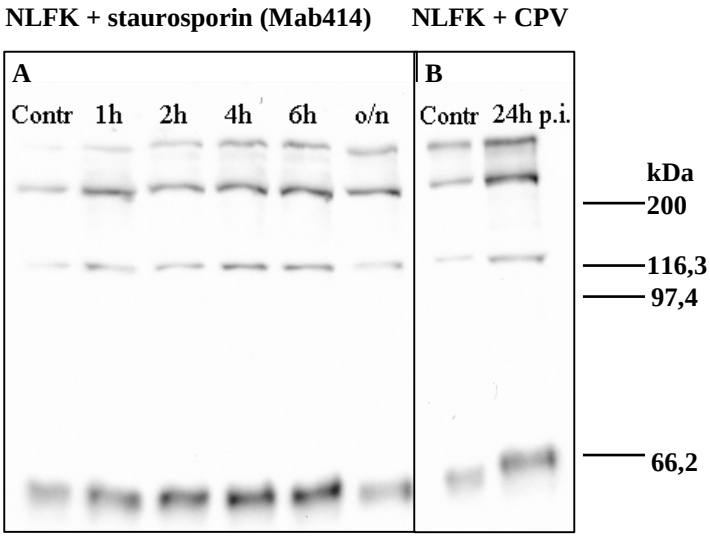

Figure 4. Nucleoporin degradation studies in NLFK cells treated with staurosporin (1μM) for inducing apoptosis (A) and in CPV infected NLFK cells (B). Western blot with Mab414 antibody labeling Nup358, Nup214, Nup153 and Nup62 showed no apoptosis or infection induced degradation of the studied nucleoporins. Nup62 as a control.

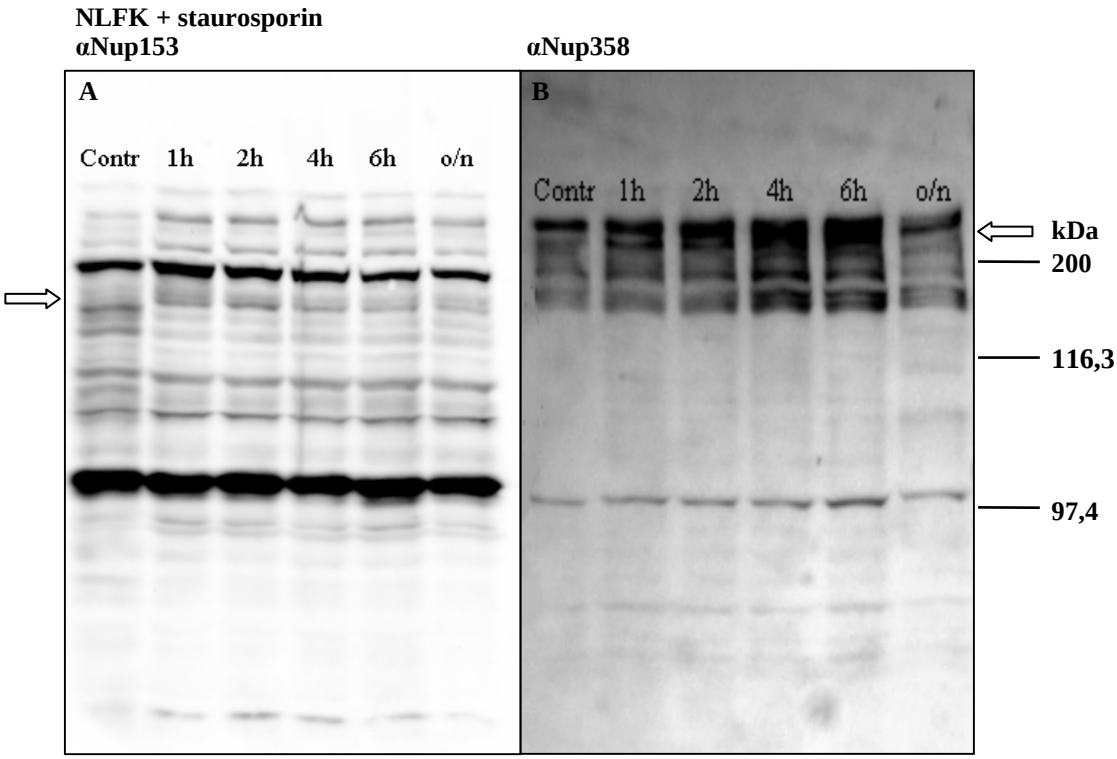

Figure 5. Staurosporin (1μM) treated NLFK cells were immunoblotted with nucleoporin specific antibodies against Nup153 (A) and Nup358 (B) (arrows) to detect possible apoptosis or CPV induced degradation. The study showed no clear degradation of the studied Nups after induction of apoptosis or as a consequence of CPV infection (data not shown).

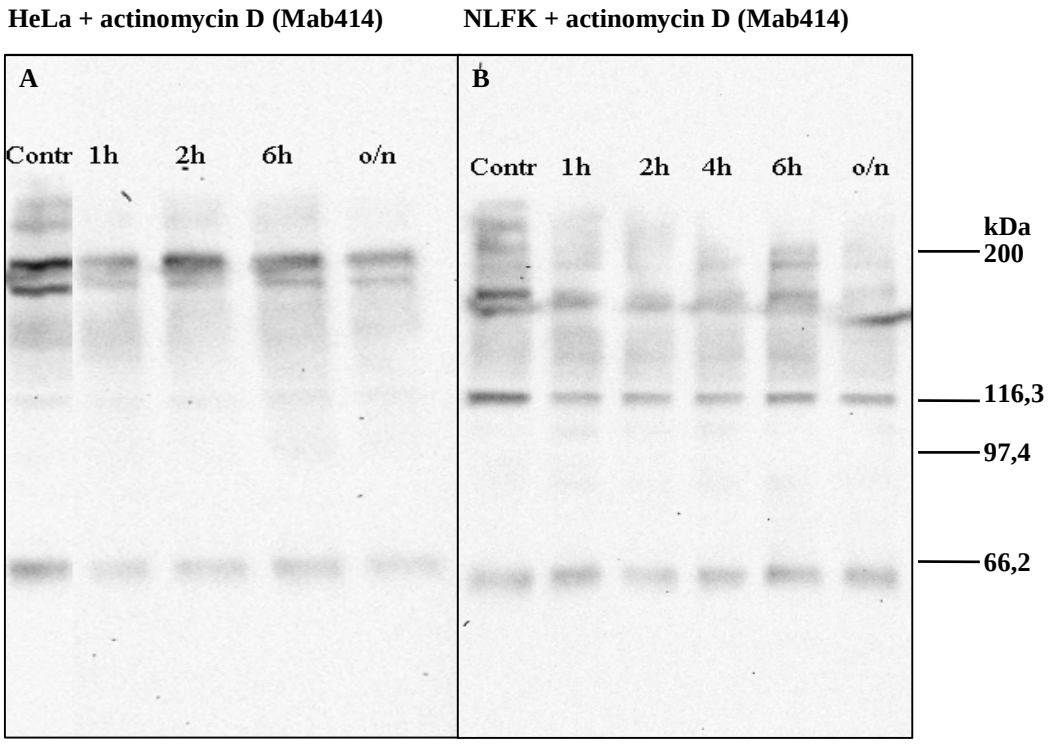

Figure 6. Western blots of HeLa (A) and NLFK (B) cells treated with actinomysin-D (0,5 µg/ml) for induction of apoptosis. Detection was accomplished with Mab414 antibody labeling nucleoporins Nup358, Nup214, Nup153 and Nup62 (control). No apparent degradation of nucleoporins was detected in apoptotic or in 24 h infected (data not shown) cells.

4.3 NE and nuclear lamin C remain unaltered in CPV infection

NLFK-LamC-EGFP cells with CPV capsids microinjected into the nuclei or cytoplasm were observed by using widefield live cell confocal microscope to record virus induced alterations in the morphology of the NE and nuclear lamin C. The observation periods were from 4 to 24 hours p.i. Several morphological changes in lamin C-EGFP were recorded during infection but all types of these changes were clearly detectable also in the non-infected control cells (Figure 7).

One of the common changes seen was a budding-like folding of the lamin towards the cytoplasm. During the cell division in control cells, lamin C fluorescence dispersed from the NE to the cytoplasm and after the division the bright fluorescence of the NE was regained through a phase in which large, bright spots appeared into the nucleus. Frequently, cells started to die after approximately 24 h p.i. In dying cells the lamins were disintegrating or undergoing dramatic morphological changes. The infected cells did not divide during observation. In this study, no sign of any clear, particularly infection induced conformational alteration of lamin C was observed (Figure 7).

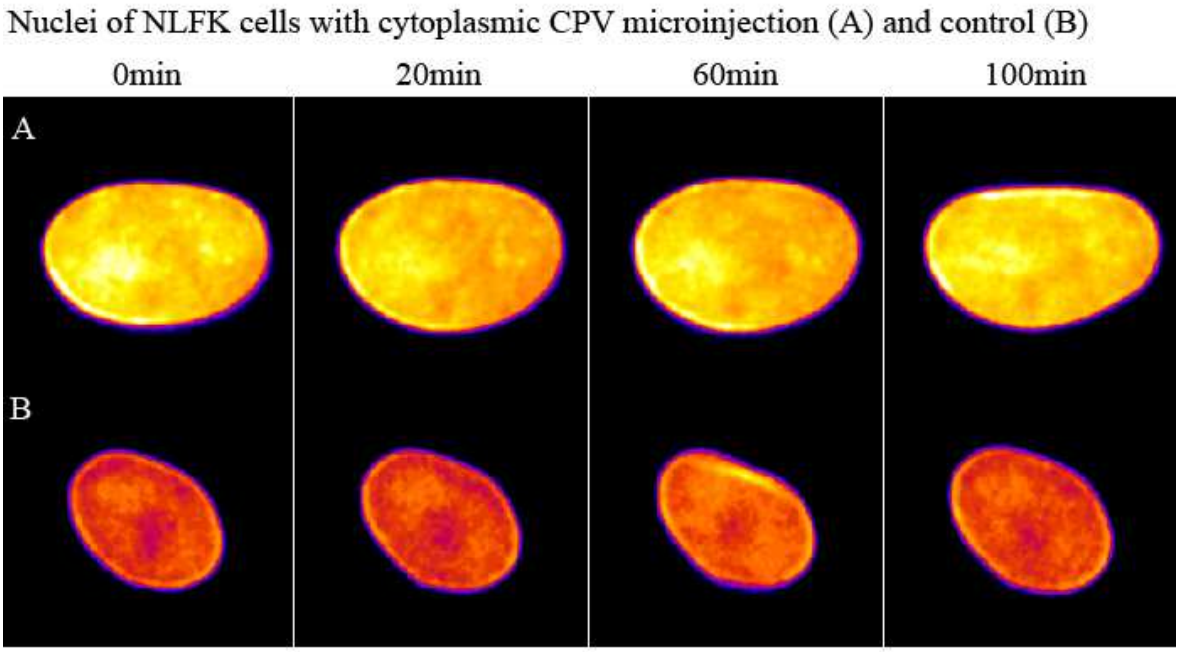

Figure 7. CPV microinjected (A) and control (B) NLFK cells stably expressing Lamin-C-EGFP visualized by live cell confocal microscope. In controls, conformational changes in the lamin were common and more frequently detected before cell division. After microinjection, similar alterations in the lamin conformation compared to the controls were detected. However, no particularly virus induced alterations were recognized. Frame rate during imaging was 12 fph.. Average intensity Z-projection pictures of 200 x 190 pixels with the pixel size of 125 µm.

In addition, the conformation of the NE and the nuclear lamin A/C was closely examined in infected, CPV microinjected and control NLFK and NLFK-LamC-EGFP cells (live and fixed). In fixed samples, fluorescent antibodies against several nucleoporins (Mab414, αTpr, Figure 9) or lamin (αlamin A/C, data not shown) did not show any detectable, particularly virus induced morphological changes in confocal microscopy. Occasionally, microinjected or infected cells with the stable LamC-EGFP expression had a throughoutly dispersed or diffuse lamin fluorescence staining in the cytoplasm. There were also no differences in the conformational behavior of the lamins in the nuclear or cytoplasmic microinjection experiments. Concentrated CPV labeling at one side of the nucleus were frequently seen in infected but not in microinjected cells. In conclusion, no verifiably virus induced changes in the conformation of the lamin A/C or the NE were encountered in this study (Figure 8,9,10).

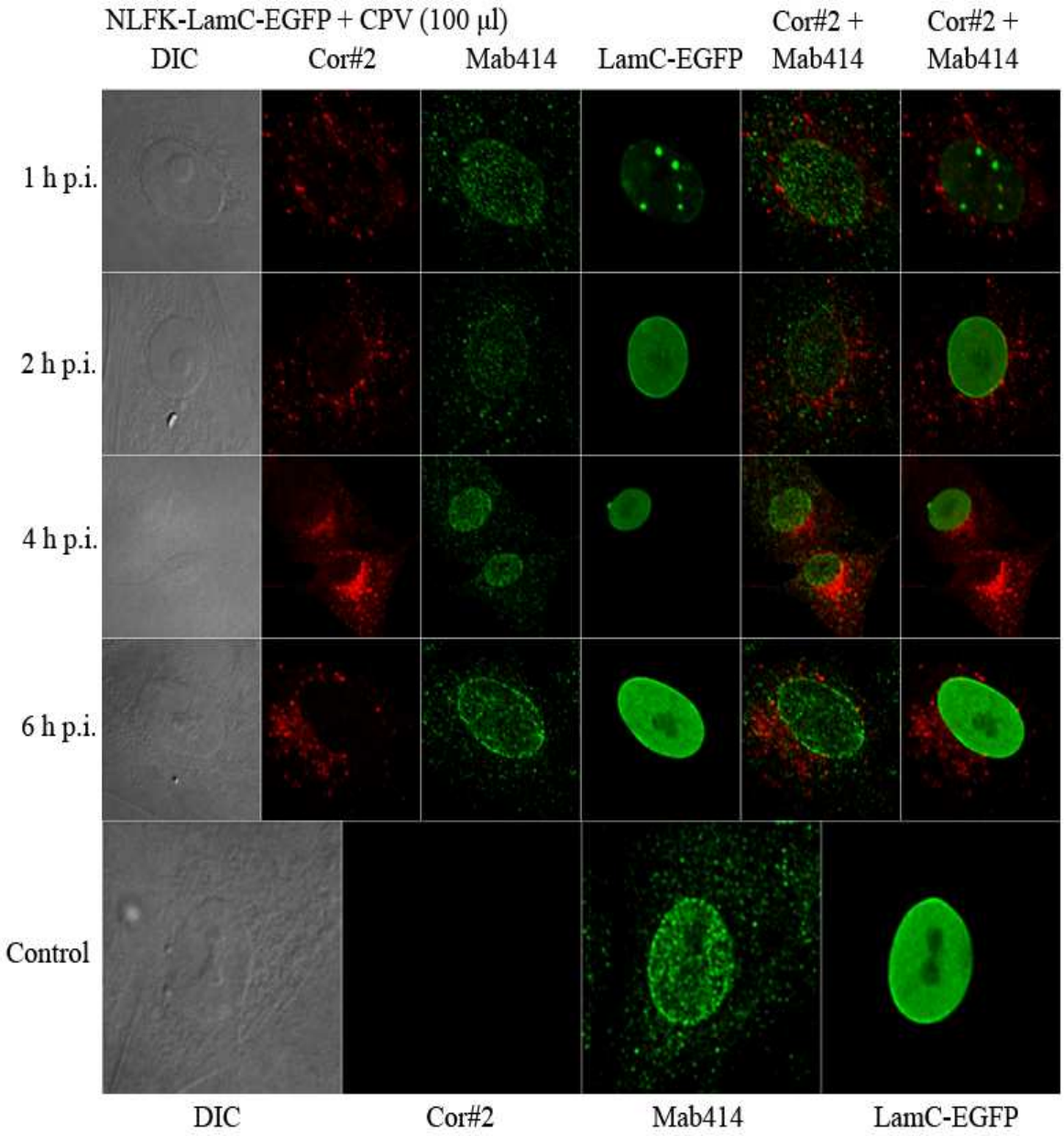

Figure 8. Control (24 h, below) and CPV infected NLFK-LamC-EGFP cells (CPV 100 µl) at 1, 2, 4, and 6 h p.i. Immunolabeling of CPV (Cornell#2, red) and certain nucleoporins (Mab414, green) showed no colocalization or specifically virus induced alterations of the NE or the nuclear lamin. Majority of CPV capsids concentrated to one side of the nucleus as infection proceeded. DIC, differential interference contrast. Confocal microscopy slice image of 800 x 800 with pixel size of 67 nm.

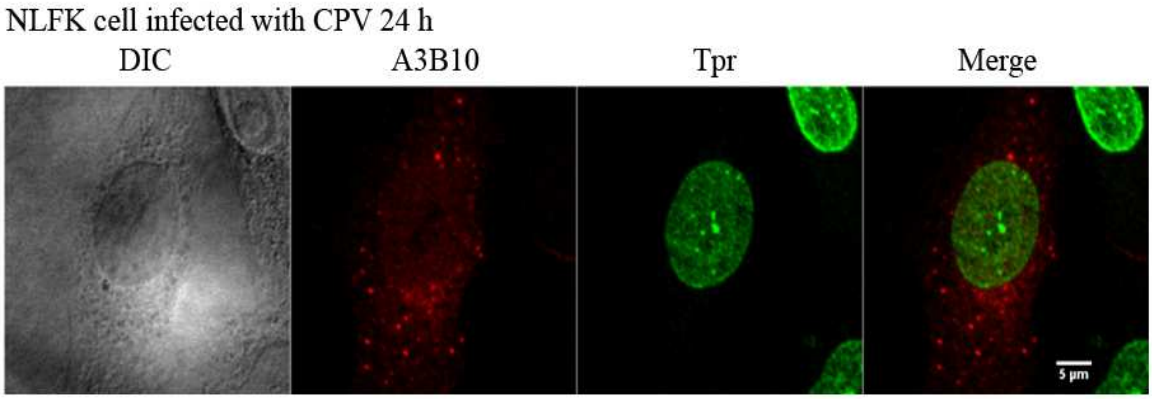

Figure 9. Confocal microscopy image of CPV infected (100 µl, 24 h p.i.) NLFK cell immunolabeled with CPV capsid antibody A3B10 (red) and nucleoporin specific antibody αTpr (green). Virus infection did not induce any detectable breaks or other significant alterations to the NE. Average intensity Z-projection, scale bar of 5 µm. DIC, differential interference contrast.

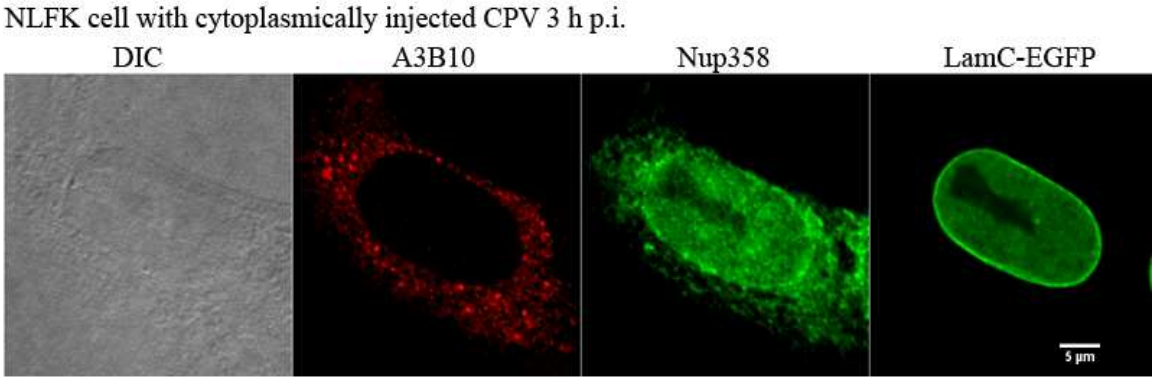

Figure 10. Confocal microscopy image of NLFK-LamC-EGFP cells with CPV microinjected to the cytoplasm (3 h p.i.). Immunolabeling was done with anti-nucleoporin antibody αNup358 (green) and CPV capsid antibody A3B10 (red). No observable, significant virus induced alterations of the lamin or the NE were recognized. Average intensity Z-projection, scale bar of 5 µm. DIC, differential interference contrast.

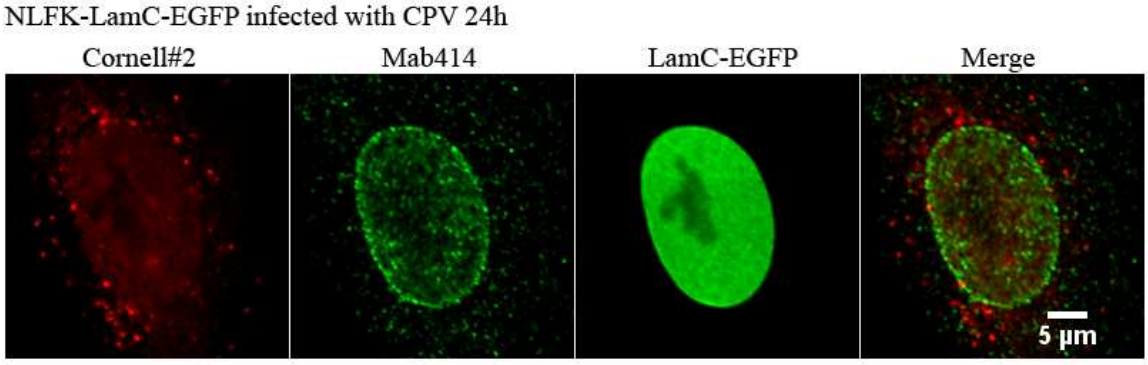

Figure 11. Single optical section confocal microscopy image of a CPV infected NLFK-LamC-EGFP (100 µl, 24 h p.i.) cell with CPV capsid proteins labeled with Cornell#2 in red and nucleoporins labeled with Mab414 in green. In addition to NE labeling, some cytoplasmic labeling with Mab414 was detected. No apparent colocalization of antibodies used was observed. Scale bar of 5 µm.

4.4 CPV-nuclear pore complex –interactions

Fixed CPV infected and control NLFK cells were immunolabeled with Nup153, Nup358 and Tpr specific antibodies, and with Mab414 labeling several nucleoporins. CPV was labeled either with antibody A3B10 or Cornell#2. Confocal microscopy was utilized. The fluorescence staining of the nucleoporins was bright and clear making the visualization of the NE possible. In addition, cytoplasmic αNup358 labeling was also detected in some extent (data not shown). In these studies, CPV did not appear to colocalize significantly with any of the nucleoporins tested in the NE, in close distance or in the cytoplasm (Figure 11).

4.5 Role of Rab1A-vesicle trafficking in CPV entry and egress

To study the cytoplasmic transport route of CPV after vesicular escape to the nucleus, Rab1A-associated vesicle trafficking was studied. The study was accomplished in CPV infected (10 min, 30 min, 1 h, 2 h, 24 h and 48 h) or Rab1A-EGFP transfected NLFK cells (24-48 h) and control cells (24-72 h). At the beginning of the infection in NLFK cells, Rab1A was mostly concentrated on one side of the nucleus in close proximity of the NE. This was also detected in the control cells. In infected NLFK cells there was no significant change in the Rab1A appearance between 10 min to 2 h p.i.. As infection proceeded, there was also some more diffuse labeling and several brighter spots of Rab1A staining in the cytoplasm. There were also no explicit changes in the appearance of Rab1A-EGFP between the cells at 24 and 48 h p.i.. Majority of the CPV capsids concentrated on the same side with the Rab1A near the NE at all time points but did not colocalize with it (Figure 12).

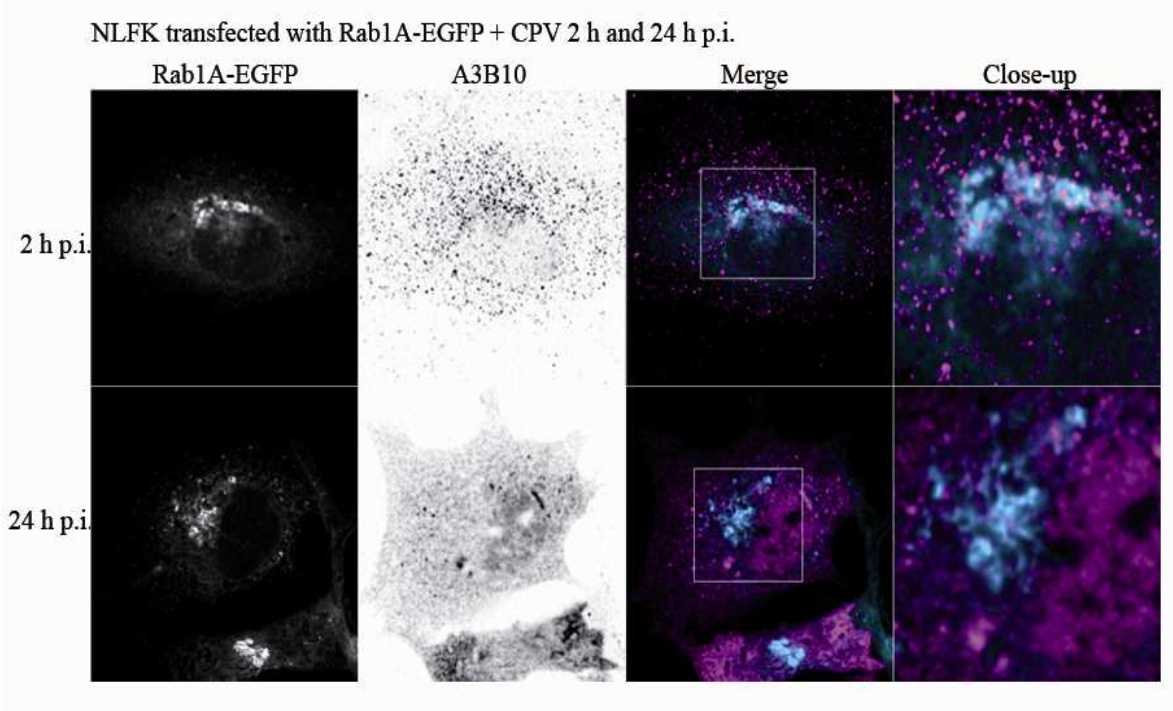

Figure 12. Rab1A-EGFP transfected and after 24 h incubation CPV infected (2 h and 24 h) NLFK cells visualized by immunolabeling of CPV capsids (A3B10) and Rab1A associated vesicles (αRab1A) for detection of colocalization. No major changes in the localization or in the appearance of the Rab1A staining was detected in this study in infection. The study showed no clear colocalization of CPV and Rab1A. Collection of maximum intensity 400 x 400 pixel images applied with Gaussian filtering (radius 1). Pixel size of 131 µm.

Viral egress was studied in pBI265 and Rab1A-EGFP transfected, TfR-negative TRVb2 cells (24-72 h post transfection, p.t.) and control cells with a confocal microscope. In control cells, the Rab1A staining localized near the NE under the nucleus and some larger, bright bundles of Rab1A fluorescent staining were also detected surrounding the NE. The same was true also for the pBI265 transfected TRVb2 cells (24 h p.tr., data not shown) without significant differences. In 72 h p.tr., the host cell death rate was high. Cells still attached to the growth surface had a more spread Rab1A fluorescence staining showing fiber or strand-like meshworks in the cytoplasm compared to cells at previous time points. In conclusion, no sign of significant colocalization of virus and Rab1A-associated vesicles was detected in this study (Figure 13).

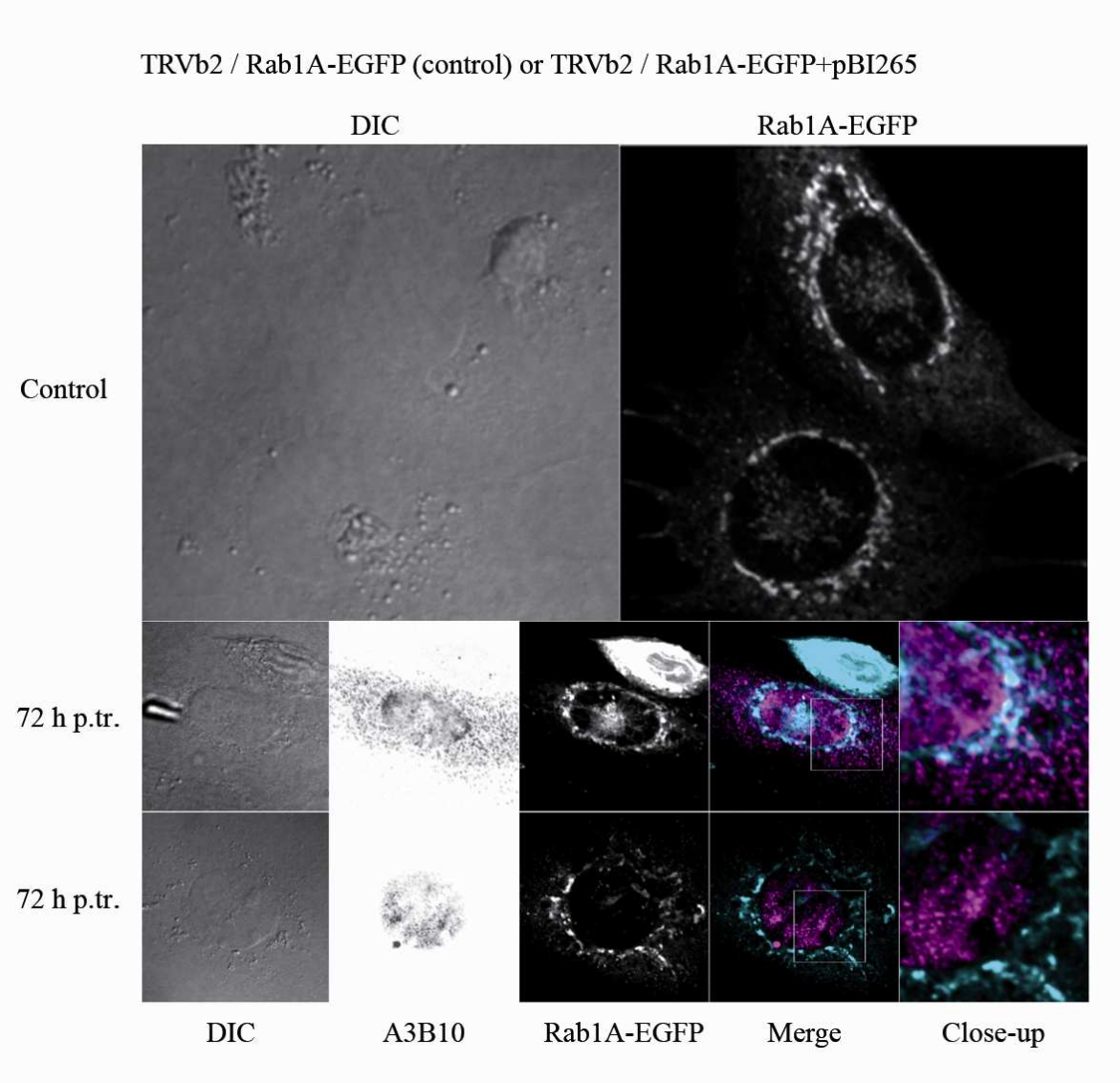

Figure 13. Rab1A-EGFP transfected (72 h) TRVb2 control cell (no pBI265, CPV clone) and Rab1A-EGFP/pBI265 dual-transfected (72 h) TRVb2 cells imaged at the putative phase of viral egress. Immunolabeling of CPV capsids (A3B10) and Rab1A associated vesicles (αRab1A). Collection of maximum intensity Z-projected images of 400 x 400 with pixel size of 176 μm. Gaussian filtering with the radius 1. DIC, differential interference contrast.

5 DISCUSSION

It has been shown that the small, autonomous CPVs enclosing a DNA genome, are imported to the nucleus via VP1-NLS –mediated route. The nuclear import is suggested to be accomplished through the NPCs with capsid interactions with importins (for review see Greber and Fassati, 2003, Vihinen-Ranta, et al., 2002). However, clear evidence for this phenomenon has not been stated. The exact events induced by this virus at the NE and the NPCs have yet remained undisclosed.

Many viruses, despite of the composition of their genomes, induce even dramatic alterations of the NE and its components during infection. Among RNA containing viruses at least the poliovirus of the *Picornaviridae* family triggers relocation of certain nuclear proteins into the cytoplasm in infection as a consequence of a rendered NE permeability through alterations of the NPC structure and function. These alterations include at least the degradation of certain nucleoporins (Nup153 and Nup62) (Belov, et al., 2004). Similar nucleoporin degradation has been shown also upon rhinovirus infection though the degradation products of the Nups differed in size compared to the poliovirus case (Gustin and Sarnow, 2002). Recent studies also present that at least one parvovirus, the MVM, induces alterations to the NE (Cohen and Panté, 2005, Nüesch, et al., 2005). MVM infection has been shown to cause damage to the NE near the NPCs in a time- and concentration-dependent manner independent of the NPCs. This suggests a mechanism in which the MVM is imported to the nucleus through the resulting breaks (Cohen and Pantè, 2005).

Based on the results stated above, it was tempting to assess the effects of CPV infection on the NE and its components through a closer examination of the NE conformation, as well as the structures of the nucleoporins and their possible colocalization with CPV in alive and fixed cells. Moreover, to get a better conception of what effects the virus induces to the NE composition, the number of the NPCs was calculated in infection and in control NLFK cells in S- or G-phase of the cell cycle in this study. In addition, the possible role of the ER intermediate compartment and Rab1A-associated vesicles was studied to assess the cytoplasmic endosomal trafficking of the CPV during its life cycle.

5.1 CPV infection does not affect the conformation of NE and lamin A/C

If viruses, like picornaviruses, with nucleus-free life cycles still have profound effects on the NE, it might not be surprising to encounter conformational NE changes derived from nuclear machinery dependent CPV. However, the results presented in this work indicate that the CPV infection in NLFK or HeLa cells does not induce notable conformational alterations of the NE, or the underlying lamins. This result supports the idea of NPC-based import of the CPV (for review see Greber and Fassati, 2003). In live-cell imaging, also no significant increase in the frequency of NE conformational alterations after introduction of the virus was visually detected in this study. Estimation of which changes in the NE or in the lamin were truly virus induced was challenging due to the amount of varied conformational changes also detectable in the control cells during normal cell growth cycle. During this research, it was also noticed that the general condition of the observed cells has a notable role in estimating if some alteration is truly infection based. It might be difficult to distinguish which alterations result in viral entry, in virus induced apoptosis and necrosis (Nykky, et al., 2010), or are due to normal cell death via apoptosis resulting from e.g. unsatisfactory growth conditions. It is also possible that the alterations were not detectable in this study due to limited resolution of the confocal microscopy and chosen methods. For acquiring factual data in the NE/lamin conformational analysis, good conditions of the sample cells, explicit microscopy and undistorted image enhancing were found to be of great significance.

5.2 Effect of CPV infection on nuclear volumes

According to the research done with αPCNA labeling, the nuclei of CPV infected NLFK cells was on average ~21 % larger than the nuclei of G-phase (G_1/G_2) non-infected cells. However, the average size of the nuclei after 24 h infection did not differ significantly from that of the S-phase control cell´s (~4 %). Volume measurements were accomplished also with αLam A/C antibody. In that study there were no significant differences in the nuclear volumes although a weak trend of increasing nuclear size was detected (Figure 12). Still, based on these results, it can be said that the nuclear volume is slightly increased in CPV infection compared to noninfected S- or G-phase cells. Nuclear size increase has been observed in earlier studies. Growth by 2.9 fold in CPV infection (24 h p.i.) has been observed by timelapse imaging of CPV infected NLFK cells (Ihalainen, et al., 2009).

Similar effect has been reported with other viruses as well. In herpes simplex 1 infection the nuclear volume at 6 h p.i. has been shown to be similar to that of mock-infected nuclei but to increase from 8 h to 16 h p.i. during viral replication by the factor of 2 (Simpson-Holley, et al., 2005). The reasons for this nuclear volume increase were not assayed in these studies but it can be speculated that this increase in infection might be due to the higher DNA content of the infected cells as was proposed by Ihalainen, et al. (2009).

In this study the nuclear size was also investigated in control cells. It can be stated that the nuclear volume increases in the S-phase during normal cell growth which is consistent with the former results (Maeshima, et al., 2010, for review see Drummond, et al., 2006, Maul, et al., 1973). With αPCNA labeling, the G-phase nuclei were found to be ~13 % smaller than the S-phase nuclei and with αLam A/C the difference was even smaller. In earlier studies, the nuclear growth in HeLa cells has been reported to increase gradually throughout the cell cycle reaching the maximum at the end of G_2 (Maeshima, et al., 2010). It might have been interesting to separate G_1 and G_2-phases also in this study to see if there was a similar trend. The used analyzing method with no separation of G_1 and G_2-phases and possible uneven amount of these samples, has affected the result and may not tell the whole truth.

5.3 CPV infection induces NE composition change

As a result of the nuclear volume growth observed in this study, there is obviously an increase of the nuclear perimeter and presumably increased total surface area of the NE. It can be speculated if the composition of NE changes in response to different metabolic situations encountered during normal cell growth. To maintain sufficient diffusion of metabolites over the NE, for instance in preparation for mitosis, the amount of NPCs changes during the cell cycle.

Indeed, formation of new pores has been shown to occur immediately after mitosis and in interphase (Antonin, et al., 2008). In addition, fluctuation of the amount of NPCs during different phases of the cell cycle has been determined in earlier studies. An increase in the amount of NPC and in the nuclear volume by the number of 2 in HeLa cells during interphase has been reported. This increase was shown to be governed by cyclin-dependent kinases whereas the nuclear growth had distinct regulation mechanisms. The researchers

stated that it seems like the nuclear volume increase does not directly trigger formation of new NPCs by showing fast increase of NPCs in G_1/S and slower increase in G_2 while the nuclear volume gradually and continuously increased (Maeshima, et al., 2010). Still, in that study the NPC density remained quite the same throughout the cell cycle as follows: 4.57 ± 0.49 NPCs per μm^2 in G_1, 5.10 ± 0.39 NPCs per μm^2 in S, and 5.43 ± 0,39 NPCs per μm^2 in G_2 (Maeshima, et al., 2010). However, the discussion of the relatedness of volume increase and NPC formation is ongoing. Studies proposing opposite results have also been published. Dultz and Ellenberg, 2010, showed those factors to be correlated in normal rat kidney cells and that the formation of new NPCs occurs at a constant rate accompanied with nuclear growth throughout the interphase. Nevertheless, these two studies agree on the constant overall NPC density during the cell cycle (Dultz and Ellenberg, 2010, Maeshima, et al., 2010). In this research, it was shown that the NPC densities of the S- and G-phase NLFK nuclei were quite similar as well as the nuclear volumes. This is consistent at least with the results of Dultz and Ellenberg, 2010. Strikingly, the NPC density in the CPV infected cells was significantly decreased, while the nuclear volume continued to increase (Figure 3, 12). It can be speculated that the CPV infection may affect either the formation of new pores, ceases it or it somehow alters the NPC structure leading to its degradation. Or it might be that the event is a summary of many: it is possible that CPV induces NE-NPC-scaffold structure breakdown accompanied with the repression of NPC biogenesis. It is supposed, that parvoviruses retain the host cell in the S-phase of the interphase (Op de Beeck and Caillet-Fauquet, 1997) where the de novo NPC biogenesis is known to take place (Chadrin, et al., 2010). Thus it can be speculated that the NPC biogenesis might be a potential target of rendering in virus infection. Moreover, the finding of this study that the studied nucleoporins known to be degraded in certain other virus infections (Belov, et al., 2004, Gustin and Sarnow, 2002) remained intact during the CPV infection, may not support the Nup degradation theory. However, in this study the induction of apoptosis did not trigger degradation of the studied Nups opposite to what was expected. This may indicate a methodological error. Even though the death rate of the cells increased after induction of apoptosis, it may still be that the chemicals used were old and therefore did not work correctly.

It has to be mentioned that in this study the NPCs were counted by computer analysis from a chosen array of optical sections of the nuclear bottom and not from the whole nucleus.

The NPC density might not be constant on different sides of the nucleus and thus these results should be treated cautiously. Nevertheless, a method using only the bottom section has been earlier discussed to be well representative for the whole nucleus (Dultz and Ellenberg, 2010). However, in this study it was recognized that further studies concentrating on the NPC density determination from the whole nucleus would be necessary for acquiring explicit information.

Normally, the NPCs are quite stable structures with life-long recidence scaffold-nucleoporins (D´Angelo, et al., 2009). Still, former studies state that the degradation of the NPCs can also be due to age-dependent deterioration through oxidative damage of several nucleoporins leading to the loss of nuclear integrity and components from the NPCs in post-mitotic cells (D´Angelo, et al., 2009). In addition, previous studies have suggested that both, parvovirus H-1 infection or merely H-1-NS1 expression, lead to increased levels of intracellular reactive oxygen species. It has also been proven that antioxidant treatment reduces this increase, cell cycle arrest, as well as apoptosis (Hristov, et al., 2010). It can be speculated if the oxygen radicals are produced and needed also in the CPV infection to increase the NPC permeability and assist the nuclear import of the virus. On the other hand, if oxidative stress is induced not until NS1 expression, it may be that this phenomenon stated above occurs only in the egress.

5.4 Nucleoporin-CPV –interactions at the NPC may be rapid

The aspect of CPV binding to the NPCs has been unclear. Nucleoporin based binding to the NPCs has been proven for example with adenovirus, which is also a DNA virus (for review see Greber and Fassati, 2003). In this study there was no notable colocalization of the studied nucleoporins (Nup153, Nup358, Tpr) and the CPV. However, due to the confocal microscope resolution it is not possible to detect single viruses at the NPCs. It may be that only one virus at a time is at the NPC in the entry interacting with these nucleoporins but this could not be detected in this study. Moreover, weather it is a question of not binding to these but to some other nucleoporin remained still unsolved. In the future, one potential target of investigation concerning this binding would be the Nup214 of the NPC cytoplasmic fibers, which has been shown to function in adenoviral nuclear import (for review see Greber and Fassati, 2003). In this study, Nup358 fluorescent staining was sometimes detected in regularly fiber-like structures in the cytoplasm. This is consistent

with former studies of Nup358 which propose a cytoplasmic presence and a role in controlling the microtubule cytoskeleton (Joseph, et al., 2004). CPV trafficking in the cytoplasm has been known to include microtubular assistance (Vihinen-Ranta, et al., 1998). Because of the presence of Nup358 in the same areas it was speculated if the CPV transport occurs attached to it. The results suggested, though, that the CPV did not bind to the Nup358 in the cytoplasmic fibers of the NPCs.

5.5 Intracellular vesicle trafficking of the CPV is not Rab1A-mediated

Because Rab1, the second isomer of Rab (Allan, et al., 2000), is involved in vesicular cytoplasmic transport and the CPV has shown to be trafficked along a vesicular route during its life cycle (Bär, et al., 2008), Rab1A was a relevant target of closer investigation.

The role of Rab1A in the viral entry was studied in infected and control NLFK cells transfected with Rab1A-EGFP. Also the possible function of Rab1A in the egress was studied in TRVb2 cells transfected with an infective CPV clone pBI265 and Rab1A-EGFP. The research done clearly showed that the CPV trafficking takes places in the same side of the nucleus and in the same area where the ERGIC is located (Scweizer, et al., 1991). This was estimated with visualizing of the Rab1A system in confocal microscopy. What also became obvious was that the CPV is not trafficked in Rab1A-associated vesicles but in a completely separate system. The future study concerning the cytoplasmic, post-endocytotic transportation of CPV could be directed still to microtubule associated vesicles or vesicles known to be involved in transferrin recycling. For example Rab11 has been shown to be required for the recycling of internalized transferrin in early endosomal compartment and thus providing a link between membrane trafficking in HeLa cells (Lindsay and Caffrey, 2002) – as one example of many.

6 CONCLUSIONS

In this thesis, the CPV infection –induced, conformational and structural alterations of the NE and the underlying lamin A/C, as well as the role of Rab1A-associated vesicles in CPV´s endosomal membrane trafficking, were investigated. The studies concerning structural alterations of the NE comprised monitoring of NPC density and possible degradation of nucleoporins Nup358, Nup214, Nup153, and Tpr with Nup62 as a control. The results suggested the interactions of the chosen Nups and CPV to be relatively rapid and temporary. It seems that CPV translocates from the cytoplasm to the nucleus via NPC mediated route since no infection induced conformational alterations e.g. breaks of the NE were detected in the study. These results are in line with former studies performed with parvoviruses. In addition, the studied Nups seemed to remain intact in infection suggesting that CPV does not induce Nup breakdown. Moreover, a small but not significant increase of nuclear volumes in CPV infection was recorded alongside with a decrease in NPC density compared to the non-infected cells in S- or G-phase of the cell cycle. The research done also proposes that the endosomal membrane trafficking of CPV does not include Rab1A-associated vesicles but occurs in the same areas of the ERGIC compartment. It might be interesting to study mechanisms behind the nuclear volume change in CPV infection. Also the phenomena behind the NPC density changes would require closer investigation. In addition, one exciting objective would be to measure the NE permeability in infection to detect possible changes. In the future, these studies might provide us a better conception of events induced by viral infection also in general.

7 REFERENCES

Abramoff, M. D., Magelhaes, P. J. and Ram, S. J. 2004. “Image processing with ImageJ”. Biophotonics International. 11: 36-42.

Alberts B., Johnson A., Lewis J., Raff M., Roberts K., Walter P. 2002. Mol Biol Cell.. 4th Edition. Garland Science. New York.

Allan, B. B., Moyer, B. D. and Balch, W. E. 2000. Rab1 recruitment of p115 into a cis-SNARE complex: programming budding COPII vesicles for fusion. Science. 289: 444-448.

Antonin, W., Ellenberg, J. and Dultz, E. 2008. Nuclear pore complex assembly through the cell cycle:Regulation and membrane organization. FEBS Letters. 582: 2004-2016. Minireview.

Appenzeller-Herzog, C. and Haurl, H-P. 2006. The ER-Golgi intermediate compartment (ERGIC): research of its identity and function. J Cell Sci.. 119: 2173-2183. Review.

Basak, S. and Compans R. W. 1989. Polarized entry of canine parvovirus in epithelial cell line. J Virol. 63: 3164-3167.

Belov, G. A., Lidsky, P. V., Mikitas, O. V., Egger, D., Lukyanov, K. A., Bienz, K. and Agol, V. 2002. bidirectional increase in permeability of nuclear envelope upon poliovirus infection and accompanying alerations of nuclear pores. J Virol. 78: 10166-10177.

Bernad, R., van der Velde, H., Fornerod, M. and Pickersgill, H. 2004. Nup358/RanBP2 attaches to the nuclear complex via association with Nup88 and Nup214/CAN and plays a supporting role in CRM-mediated nuclear protein export. Mol Cell Biol.. 24: 2373-2384.

Bär, S., Daeffler, L., Rommelaere, J. and Nüesch, J. P. F. 2008. Vesicular egress of non-enveloped lytic parvoviruses depends on gelsolin functioning. PLos Pathog. 4(8): e1000126.

Chardin, A., Hess, B., San Roman, M., Gatti, X., Lombard, B., Loew, D., Barral, Y., Palancade, B. and Doye, V. 2010. Pom33, a novel transmembrane nucleoporin required for proper nuclear pore complex distribution. J Cell Biol. 189: 795-811.

Chang, SF., Sgro, JY. and Parrish, C. R. 1992. Multiple amino acids in the capsid structure of canine parvovirus coordinately determine the canine host range and specific antigenic and hemagglutination properties. J Virol. 66: 6858-6867.

Christensen, J. and Tattersall, P. 2002. Parvovirus initiator protein NS1 and RPA coordinate replication fork progression in a reconstituted DNA replication system. J Virol. 76: 6518-6531.

Christensen, J., Cotmore, S. F. and Tattersall, P. 1997. A novel cellular site-specific DNA-binding protein cooperates with the viral NS1 polypeptide to initiate parvovirus DNA replication. J Virol. 71: 1405-1416.

Cohen, S. and Pantè, N. 2005. Pushing the envelope: microinjection of Minute virus of mice into Xenopus oocytes causes damage to the nuclear envelope. J Gen Virol. 86: 3243-3252.

Cotmore, S. F. and Tattersall, P. 1998. High-mobility-group 1/2 proteins are essential for initiating rolling-circle –type DNA replication at a parvovirus hairpin origin. J Virol. 74: 8477-8484.

Cotmore, S. F. and Tattersall, P. 1988. The NS1 polypeptide of minute virus of mice is covalently attached to the 5´termini of duplex replicative form DNA and progeny single strands. J Virol. 62: 851-860.

Cotmore, S. F. and Tattersall, P. 1987. The autonomously replicating parvoviruses of vertebrates. Adv Virus Res. 33: 91–174.

Cziepluch, C., Lampel, S., Grewenig, A., Grund, C., Lichter, P. and Rommelaere, J. 2000. H-1 parvovirus-associated replication bodies: a distinct virus-induced nuclear structure. J Virol. 74: 4807-4815.

D´Angelo, M. A, Raices, M., Panowski, S. H. and Hetzer, M. W. 2009. Age-dependent detorioration of nuclear pore complexes causes aloss of nuclear integrity in post-mitotic cells. Cell. 23: 284-295.

Drummond, S. P., Rutherford, S. A., Sanderson, H. S. and Allen, T. D. 2006. High resolution analysis of mammalian nuclear structure throughout the cell cycle: implications for nuclear pore complex assembly during interphase and mitosis. Can J Physiol Pharmacol. 84: 423-430. Review.

Dultz, E. and Ellenberg, J. 2010. Live imaging of single nuclear pore reveals unique assembly kinetics and mechanism in interphase. J Cell Biol. 191: 15-22.

Fahrenkrog, B., Köser, J. and Aebi, U. 2004: The nuclear pore complex: a jack of all trades? Trends Biochem Sci. 29:. 175-182. Review.

Farr, G. A., Zhang, L. and Tattersall, P. 2005. Parvoviral virions deploy a capsid-tethered lipolytic enzyme to breach the endosomal membrane during cell entry. PNAS. 102: 17148-17153.

Fried, H. and Kutay, U. 2003. Nucleocytoplasmic transport: taking an inventory. Cell Mol Life Sci. 60: 1659-1688. Review.

Frosst, P., Tinglu, G., Subauste, C., Hahn, K. and Gerace, L. 2002. Tpr is localized within the nuclear basket of the pore complex and has a role in nuclear protein export. J Cell Biol. 156: 617-630.

Gerace, L. and Blobel, G. 1982. Nuclear lamina and the structural organization of the nuclear envelope. Cold Spring Harb Symp Quant Biol. 46: 967-978.

Gerace, L. and Burke, B. 1988. Functional organization of the nuclear envelope. Annu Rev Cell Biol. 4: 335-374.

Greber, U. F. and Fassati, A. 2003. Nuclear import of viral DNA genomes. Traffic. 4: 136-143. Review.

Gruenbaum, Y., Margalit, A., Goldman, R. D., Shumaker, D. K. and Wilson, K. L. 2005. The nuclear lamina comes of age. Nat Rev Mol Cell Biol. 6: 21-31.

Gustin, K. E. and Sarnow, P. 2002. Inhibition of nuclear import and alternation of nuclear pore complex composition. J Virol. 76: 8787-8796.

Harbison, C. E., Lyi, S. M., Weichert, W. and Parrish, C. R. 2009: Early steps in cell infection by parvoviruses: host-spesific differences in cell receptor binding but similar endosomal trafficking. J Virol.. 83: 10504-10514.

Harbison, C. E., Chiorini, J. A. and Parrish, C. R. 2008. The parvovirus capsid odyssey: from the cell surface to the nucleus. Trends Microbiol.. 16. 208-214.

Hase, M. E. and Cordes, V. C. 2003. Direct interaction with Nup153 mediates binding of Tpr to the periphery of the nuclear pore complex. Mol Biol Cell. 14: 1923-1940.

Heessen, S. and Fornerod, M. 2007. The inner nuclear envelope as a transcription factor resting place. EMBO reports (2007). 8: 914-919. Review.

Herrero, Y. C. M., Cornelis, J. J., Herold-Mende, C., Rommelaere, J., Schlehofer, J. R. and Geletneky, K. 2004. Parvovirus H-1 infection of human glioma cells leads to complete viral replication and efficient cell killing. Int J Cancer. 109: 76-84.

Hetzer, M. W., Walther, T. C. and Mattaj, I. W. 2005. Pushing the envelope: structure, function and dynamics of the nuclear periphery. Annu Rev Cell Dev Biol. 21: 347-380. Review.

Hristov, G., Krämer, M., Li, J., El-Andaloussi, N., Mora, R., Daeffler, L., Zentgraf, H., Rommelaere, J. and Marchini, A. 2010. Through its nonstructural protein NS1, parvovirus H-1 induces apoptosis via accumulation of reactive oxygen species. J Virol. 84: 5909-5922.

Hueffer, K., Parker, J. S. L., Weichert, W., Geisel, R., Sgro, J-Y. and Parrish, C. 2003. The natural host range shift and subsequent evolution of canine parvovirus resulted from virus-spesific binding to the canine transferrin receptor. J Virol. 77: 1718-1726.

Ihalainen, T. O., Niskanen, E. A., Jylhävä, J., Turpeinen, T., Rinne, J., Timonen, J. and Vihinen-Ranta, M. 2007. Dynamics and interactions of parvoviral NS1 protein in the nucleus. Cell Microbiol. 9(8): 1946-1959.

Ihalainen, T. O., Niskanen, E. A., Jylhävä, J., Paloheimo, O., Dross, N., Smolander, H., Langowski, J., Timonen, J. and Vihinen-Ranta, M. 2009. Parvovirus induced alterations in nuclear architecture and dynamics. Plos One 4: e5948.

Joseph, J. and Dasso, M. 2008. The nucleoporin Nup358 associates with and regulates interphase microtubules. FEBS Letters. 582: 190-196.

Joseph, J., Liu, S. T., Jablonski, S. A., Yen, T. J. and Dasso, M. 2004. The Ran-GAP1-RanBP2 complex is essential for microtubule-kinetochore interactions in vivo. Curr Biol. 14: 611-617.

Kiseleva, E., Rutherford, S., Cotter, L. M., Allen, T. D. and Goldberg, M. W. 2001. Steps of nuclear pore disassembly and reassembly during mitosis in early Drosophila embryos. J Cell Sci. 114: 3607-3618.

Krull, S., Dörries, J., Boysen, B., Reidenbach, S., Magnius, L., Norder, H., Thyberg, J. and Cordes, V. C. 2010. Protein Tpr is required for establishing nuclear pore-associated zones of heterochromatin exclusion. The EMBO journal. 29: 1659-1673.

Krull, S., Thyberg, J., Björkroth, B., Rackwitz, H. and Cordes, V. C. 2004. Nucleoporins as components of the nuclear pore complex core structure and Tpr as the architectural element of the nuclear basket. Mol Biol Cell. 15: 4261-4277.

Lachmann, S., Rommelaere, J. and Nuesch, J. P. 2003. Novel PKCη is required to activate replicative functions of the major nonstructural protein NS1 of minute virus of mice. J Virol. 77:8048-8060.

Lee, J. S. H., Hale, C. M., Panochran, P., Khatau, S. B., George, J. P., Tseng, Y., Stewart, C. L., Hodzic, D. and Wirtz, D. 2007. Nuclear lamin A/C deficiency induces defects in cell mechanics, polarization and migration. Biophys J. 93: 2542-2552.

Lindsay, A. J. and Caffrey, M. W. 2002. Rab11-FIP2 functions in transferrin recycling and associates with endosomal membranes via its COOH-terminal domain. J Biol Chem. 277: 27193-27199.

Maeshima, K., Iino, H., Hihara, S., Funakoshi, T., Watanabe, A., Nishimura, M., Nakatomi, R., Yahata, K., Imamoto, F., Hashikawa, T., Yokota, H. and Imamoto, N. 2010. Nuclear pore formation but not nuclear growth is governed by cyclin-dependent kinases (Cdks) during interphase. Nat Struct Mol Biol. 17: 1065-1071.

Maul, G. G., Maul, H. M., Scogna, J. E., Lieberman, M. W., Stein, G. S., Hsu, B. Y. and Borun, T. W. 1972. Time sequence of nuclear pore formation in phytohemagluttinin-stimulated lymphocytes and HeLa cells during the cell cycle. J Cell Biol. 55: 433-447.

Maul, H. M., Yee-Li Hsu, Betty, Borun, T. M. and Maul, G. G. 1973. Effect of metabolic inhibitors on nuclear pore formation during the HeLa S_3 cell cycle. J Cell Biol. 59: 669-676.

McGraw, T. E., Greenfield, L. and Maxfield F. R. 1987. Functional expression of the human transferrin receptor cDNA in Chinese hamster ovary cells deficient in endogenous transferrin receptor. J Cell Biol. 105: 207-214.

Mitchell, P. J. and Cooper, C. S. 1992. The human Tpr gene encodes a protein of 2094 amino acids that has extensive coiled-coil regions and an acidic C-terminal domain. Oncogene. 7: 2329-2333.

Nüesch, J. P. and Rommelaere, J. 2006. NS1 interaction with CKII alpha: Novel protein complex mediating parvovirus-induced cytotoxicity. J Virol.. 80: 4729-4739.

Nüesch, J. P. F., Lachmann, S., and Rommelaere, J. 2005. Selective alterations of the host cell architecture upon infection with parvovirus minute virus of mice. Virology. 331: 159-174.

Nykky, J., Tuusa, J. E., Kirjavainen, S., Vuoneto, M. and Gilbert, L. 2010. Mechanisms of cell death in canine parvovirus-infected cells provide intuitive insights to developing nenotools for medicine. Int J Nanomedicine. 5: 417-428.

Paine, P. L., Moore, L. C. and Horowitz, S. B. 1975. Nuclear envelope permeability. Nature. 254: 109-114.

Pakkanen, K., Nykky, J. and Vuento, M. 2008. Late steps of parvoviral infection induce changes in cell morphology. Virus Res. 137: 271-274. Short communication.

Pantè, N. and Kann, M. 2002. Nuclear pore complex is able to transport macromolecules with diameters of about 39 nm. Mol Biol Cell. 13: 425-434.

Parker, J. S. and Parrish, C. R. 1997. Canine parvovirus host range is determined by the specific conformation of an additional region of the capsid. J Virol. 71: 9214-9222.

Parker, J. S. and Parrish, C. R. 2000. Cellular uptake and infection by canine parvovirus involves rapid dynamin-regulated clathrin-mediated endocytosis, followed by slower intracellular trafficking. J Virol. 74:1919-1930.

Parker, J. S. L., Murphy, W. J., Wang, D., O´Brien, S. J., and Parrish, C. R. 2001. Canine and feline parvoviruses can use human or feline transferring receptors to bind, enter and infect cells. J Virol. 75: 3896-3902

Parrish, C. R. 1991. Pathogens of feline panleukopenia virus and canine parvovirus. Baillieres Clin Haematol. 8: 57-71.

Reed, A. P., Jones, E.V., and Miller, T. J. 1988. Nucleotide sequence and genome organization of canine parvovirus. J Virol. 62: 266-276.

Scmitz, A., Schwarz, A., Foss, M., Zhou, L., Rabe, B., Hoellenriegel, J., Stoeber, M., Pantè, N. and Kann, M. 2010. Nucleoporin 153 arrests the nuclear import of Hepatitis B virus capsids in the nuclear basket. PloS Pathog. 6(1): e1000741.

Schweizer, A., Matter, K., Ketcham, C. M. and Hauri, H. P. 1991. The isolated ER-Golgi intermediate compartment exhibits properties that are different from ER and cis-Golgi. J Cell Biol. 113: 45-54.

Shah, S., Tugendreich, S. and Forbes, D. 1998. Major binding sites for the nuclear import receptor are the integral nucleoporin Nup153 and the adjacent nuclear filament protein Tpr. J Cell Biol. 141: 31-49.

Simpson-Holley, M., Colgrove, R. C., Nalepa, G., Harper, J. and Knipe, D. 2005. Identification and Functional Evaluation of Cellular and Viral Factors Involved in the Alteration of Nuclear Architecture during Herpes Simplex Virus 1 Infection. J Virol. 79: 12840-12851.

Stewart, C. L., Roux, K. J. and Burke, B. 2007. Blurring the boundary: the nuclear envelope extends its reach. Science. 318: 1408-1412.

Stoffler, D., Fahrenkrog, B. and Aebi, U. 1999. The nuclear pore complex: from molecular architecture to functional dynamics. Cell Biol. 11: 391-401.

Suikkanen, S., Sääjärvi, K., Hirsimäki, J., Välilehto, O., Reunanen, H., Vihinen-Ranta, M., and Vuento, M. 2002. Role of recycling endosomes and lysosomes in dynein-dependent entry of canine parvovirus. J Virol. 76: 4401-4011.

Suikkanen, S., Antila, M., Jaatinen, A., Vihinen-Ranta, M., and Vuento, M. 2003I. Release of canine parvovirus from endocytic vesicles. Virology. 316: 267-280.

Suikkanen, S., Aaltonen, T., Nevalainen, M., Välilehto, O., Lindholm, L., Vuento, M., and Vihinen-Ranta, M. 2003II. Exploitation of microtubule cytoskeleton and dynein during parvoviral traffic toward the nucleus. J Virol. 77:10270-10279.

Trowbridge, I. S., and Shackelford, D. A. 1986. Structure and function of transferrin receptors and their relationship to cell growth. Biochem Soc Symp. 51:117–129.

Truyen, U., and C. R. Parrish**.** 1992. Canine and feline host ranges of canine parvovirus and feline panleukopenia virus: distinct host cell tropisms of each virus in vitro and in vivo. J Virol. 66:5399–5408.

Tsao, J., Chapman, M. S., Agbandje, M., Keller, W., Smith, K., Wu, H., Luo, M., Smith, T. J., Rossmann, M. G., et al. 1991. The three-dimensional structure of canine parvovirus and its functional implications. Science. 251: 1456-1464.

Vihinen-Ranta, M., Wang, D., Weichert, W. S. and Parrish, C. R. 2002. The VP1 N-terminal sequence of canine parvovirus affects the nuclear transport of capsids and efficient cell infection. J Virol. 76(4): 1884-1891.

Vihinen-Ranta, M., Yuan, M. W. and Parrish, C. R. 2000. Cytoplasmic trafficking of the canine parvovirus capsids and its role in infection and nuclear transport. J Virol. 74: 4853-4859.

Vihinen-Ranta, M., Kalela, A., Mäkinen, P., Kakkola, L., Marjomäki, V. and Vuento, M. 1998. Intracellular route of canine parvovirus entry. J Virol. 72: 802-806.

Vogt, T. M., Blackwell, A. D., Giannetti, A. M., Bjorkman, P. J. and Enns, C. A. 2003. Heterotypic interactions between transferrin receptor and transferrin receptor 2. Blood. 101: 2008-2014.

Walther, T. C., Pickersgill, H. S., Cordes, V. C., Goldberg, M. W., Allen, T. D., Mattaj, I. W. and Fornerod, M.. 2002. The cytoplasmic filaments of the nuclear pore complex are dispensable for selective nuclear protein import. J Cell Biol. 158: 63-77.

Weichert, W. S., Parker, J. S., Wahid, A. T. M., Chang, S., Meier, E. and Parrish, C. R. 1998. Assaying for structural variation in the parvovirus capsid and its role in infection. Virology. 250: 106-117.

Willwand, K., Baldauf, A. Q., Deleu, L., Mumtsidu, E., Costello, E., Beard, P. and Rommelaere, J. 1997. The minute virus of mice (MVM) nonstructural protein NS1 induces nicking of MVM DNA at unique site of the right-end telomere in both hairpin and duplex conformations in vitro. J Gen Virol. 78: 2647-2655.

Xie, Q. and Chapman, M. S. 1996. Canine parvovirus capsid structure, analyzed at 2.9 Å resolution. J Mol Biol. 264: 497-520.

APPENDICES

Appendix I: Solutions and Reagents

50 x TAE-buffer

212 g Tris

57,1 ml acetic acid

100 ml 0.5 M EDTA, pH 8

Diluted to 1 l of H_2O

1 x TAE-buffer is prepared by 1:50 dilution in H_2O

Mowiol-DABCO

20 g Mowiol

80 ml PBS

40 ml 100 % glyserol

25 x PBS

200 g NaCl

5 g KCl

5 g KH_2PO_4

36,2 g NA_2HPO_4 x $2H_2O$

Diluted in 1 l of H_2O

1 x PBS is prepared by 1:25 dilution in H_2O

BSA-PBS

1 g Bovine Serum Albumine (BSA)

Diluted in 100 ml PBS

4% PFA-PBS

4 g paraformaldehyde (Merc, Darmstadt, Germany)

Diluted in 100 ml PBS